IEEE Access
Multidisciplinary ⋮ Rapid Review ⋮ Open Access Journal

Received February 2, 2022, accepted March 3, 2022, date of publication March 8, 2022, date of current version March 16, 2022.

Digital Object Identifier 10.1109/ACCESS.2022.3157634

Overview of Planar Antenna Loading Metamaterials for Gain Performance Enhancement: The Two Decades of Progress

BASHAR A. F. ESMAIL[1], (Member, IEEE), SLAWOMIR KOZIEL[1], (Fellow, IEEE), AND STANISLAW SZCZEPANSKI[2]

[1]Department of Engineering, Reykjavik University, 102 Reykjavik, Iceland
[2]Faculty of Electronics, Telecommunications and Informatics, Gdańsk University of Technology, 80-233 Gdańsk, Poland

Corresponding author: Bashar A. F. Esmail (basharf@ru.is)

This work was supported in part by the Icelandic Centre for Research (RANNIS) under Grant 217771, and in part by the National Science Centre of Poland under Grant 2018/31/B/ST7/02369.

ABSTRACT Metamaterials (MTMs) are artificially engineered materials with unique electromagnetic properties not occurring in natural materials. MTMs have gained considerable attention owing to their exotic electromagnetic characteristics such as negative permittivity and permeability, thereby a negative refraction index. These extraordinary properties enable many practical applications such as super-lenses, and cloaking technology, and are used to design different electromagnetic devices like filters, polarization converters, sensors, and absorbers. Advances in MTMs have made new application fields to emerge in communication subsystems, especially in the field of antennas. MTMs are usually arranged in front or above the radiating element, or incorporated in the same substrate to improve the performance of planar antennas, in terms of improving directivity, gain, bandwidth, and efficiency, reducing the size and mutual coupling, and deflecting the radiation characteristics. High gain antennas are demanded in modern wireless communication systems. Their importance is in improving the signal strength by reducing the interference and alleviating the free space path loss. This review paper provides a brief introduction to MTMs, with the focus on their operating principles. Furthermore, a detailed study of antenna gain enhancement based on the various properties of MTMs is carried out. MTMs with low values of constitutive parameters; zero-index material (ZIM), low-index material (LIM), epsilon-near-zero (ENZ), and mu-near-zero (MNZ) are discussed in detail in the context of their capability to enhance the gain of a broad class of planar antennas. The low impedance property and lensing property, which is achieved by three different characteristics: high refractive index (HRI), gradient refractive index (GRIN), and negative refractive index (NRI) materials, are loaded to planar antennas for gain enhancement. The scope of this review has been limited to antennas that were experimentally validated in the respective source papers.

INDEX TERMS Metamaterials (MTMs), gain enhancement, low impedance MTM, MTM lens, planar antennas, ZIM.

I. INTRODUCTION

Metamaterials (MTMs) are generally defined as artificially engineered materials with distinctive effective medium properties that are not naturally obtainable. Over the last two decades, these materials attracted considerable attention due to their extraordinarily electromagnetic characteristics such as negative permittivity ε, permeability μ, and index of refraction [1], [2]. These media are arranged as periodic unit cells whose average size is significantly shorter than the guided wavelength λ_g, specifically around $\lambda_g/4$. The first demonstration of the irregular electromagnetic response of the MTM, which exhibits simultaneously negative ε and μ, was performed in the theoretical study by Veselago in 1968 [3]. After almost three decades, Pendry *et al.* proposed the effective medium theory to enable a construction of such materials [4], [5]. In 2000, the first MTM structure consisting of split-ring resonators (SRR) and metallic

The associate editor coordinating the review of this manuscript and approving it for publication was Debdeep Sarkar.

cut wires was experimentally verified by Smith *et al.* [6]. MTMs with these basic properties can be utilized as a part of essential applications that include but are not limited to super-lenses [7], [8], cloaking technology [9]–[11], and subwavelength resolution and focusing [12], [13]. Moreover, these artificial structures are widely used to design different electromagnetic devices such as filters, polarization converters, and absorbers [14]–[16]. However, the inherent losses of these materials affect the performance of such devices. Consequently, several studies were conducted to investigate and reduce these losses at different frequency bands [17]–[19].

Advances in MTMs have enabled new application areas in communication subsystems, especially in the antenna technology. Since the appearance of MTMs, the researchers in the antenna engineering community have immediately acknowledged the significance of their unusual electromagnetic properties, which can be used to enhance the performance of a wide variety of the antennas, in terms of improving directivity, gain, impedance bandwidth, and efficiency, reducing the size, deflecting the radiation characteristics, and reducing the mutual coupling in multiple-input-multiple-output (MIMO) antennas [20]–[27]. Furthermore, the antenna array inspired by the MTMs was used for microwave medical imaging applications, where the radiation elements of the antenna array were utilized as biosensors to detect malignant tumors in breasts [28].

In this review, a particular emphasis will be put on the enhancement of antenna gain based on various characteristics of MTMs. The term antenna gain defines the degree to which an antenna concentrates radiated power in a given direction, or absorbs incident power from that direction, compared with a reference antenna. By improving the gain performance, the ability of antennas to communication over large distances can be enhanced as well.

High-gain planar antennas are usually preferred in modern communications systems, whether installed on terrestrial locations or based on satellites. With the advent of fifth-generation (5G) wireless communications, the frequency of operation significantly increased to millimeter-wave spectra such as 28 GHz, 38 GHz, and 60 GHz [29]. However, based on Friis's formula, these frequencies experience high free-space path loss, thereby providing short-range communications compared to the fourth-generation (4G) band. To combat this loss, the high-gain directional antennas are utilized at both ends of the communication system [30], [31]. In this regard, MTMs are strong candidates to realize 5G antennas of required characteristics.

Several methods have been proposed in the literature for enhancing the performance of planar antennas in terms of gain and directivity, some of which include: (i) arranging planar antennas in an array configuration [32], [33], (ii) loading a reflector layer [34], [35], (iii) utilization of shorting pins to optimize the impedance matching of the planar antenna [36], [37], (iv) employing high permittivity substrates [38], [39], (v) altering the basic shape of the antenna [40], [41], (vi) utilizing multiple substrates [42], [43], (vii) loading artificial materials such as Frequency Selective Surface (FSS) [44]–[46], Electromagnetic Band-Gap (EBG) [47], [48], Metasurfaces [49], [50], or Artificial Magnetic Conductor (AMC) [51], [52]. However, most of these approaches have drawbacks, such as bulky structures, they are complex and often difficult to fabricate, require complicated power distribution, exhibit narrow bandwidth, etc. Integrating MTM with planar antennas does not demand a complicated feed or power distribution system to achieve high gain as compared to conventional array antennas [53], [54].

A comprehensive study on the concept and theory of MTM transmission-line and its applications in the antenna field was presented in [55]. MTM transmission-line include series left-handed capacitances (C_L), shunt left-handed inductances (L_L), series right-handed inductances (L_R), and shunt right-handed capacitances (C_R) that are realized by slots or interdigital capacitors, stubs or via-holes, unwanted current following on the surface, and gap distance between the surface and ground-plane, respectively. In this survey, the critical features of a wide range of MTM structures were studied, and their effects on the antenna's performance were discussed in terms of size, impedance bandwidth, gain, efficiency, and simplicity. Another survey, on the other hand, focused on mutual-coupling reduction methods based on the MTM and metasurface in antenna array for MIMO and synthetic aperture radar (SAR) applications [56]. This work showed that MTM and metasurface can provide a higher level of isolation between neighbouring radiating elements using easily realizable and cost-effective structures without affecting the system size and performance, such as the bandwidth, gain and efficiency. To the best of our knowledge, no reported survey is carried out in the literature to discuss the employment of MTMs for achieving high gain antennas. This work provides the latest diverse techniques available to improve the antenna gain based on MTMs. MTM structures with low values of constitutive parameters; zero-index material (ZIM), low-index material (LIM), epsilon-near-zero (ENZ), and mu-near-zero (MNZ) were proposed in the literature to increase the gain of planar antennas. Moreover, other properties were also used for obtaining high gain antennas, such as low impedance MTM, and MTM lenses based on gradient refractive index (GRIN), and negative refractive index (NRI).

This review is organized as follows: The classification of the MTMs based on their constitutive parameters is presented in Section II. A detailed study of the gain enhancement of planar antennas using MTMs is presented in Section III, where different properties of MTMs such as the ZIM, ENZ, MNZ, low impedance, and lensing properties of MTMs are utilized for achieving high gain performance. Section IV concludes the paper.

II. MTM CLASSIFICATION

The two fundamental quantities, the electric ε, and magnetic μ, also known as the constitutive parameters, are used to describe the electromagnetic wave nature and its behavior in a medium. These parameters and the boundary conditions

demonstrate the response of the medium to an incoming electromagnetic wave. The electromagnetic characteristics of an MTMs can be expressed by the Lorentz-Drude model with two frequency-dependent macroscopic parameters, $\varepsilon_r(\omega)$ and $\mu_r(\omega)$, as follows [57], [58]:

$$\varepsilon_r(\omega) = 1 - \frac{\omega_{pe}^2}{\omega^2 - \omega_{0,\mathrm{e}}^2 + \mathrm{i}\omega\gamma_\mathrm{e}} \tag{1}$$

$$\mu_r(\omega) = 1 - \frac{\omega_{pm}^2}{\omega^2 - \omega_{0,m}^2 + i\omega\gamma_m} \tag{2}$$

where $\omega_{0,e}$ and $\omega_{0,m}$ are the transverse resonance frequency, $\omega_{pe}(\omega_{pm})$ is the electric (magnetic) coupling strength, γ_e and γ_m are the damping factors (material losses). The classification of MTMs relies on the signs of the ε and μ of a homogeneous material. The material properties can be characterized over a wide frequency range using proper values in (1) and (2). According to Veselago, when both ε and μ are simultaneously negative, some unusual phenomena occur, such as reversed Snell Law, Cerenkov radiation, and Doppler shift [59]–[61]. The material classifications based on ε and μ with the electromagnetic wave interacting with four possible materials are depicted in Fig. 1. The materials with both ε and μ are positive are known as double-positive (DPS) materials, which include the majority of conventional dielectric materials. This type is shown in the top-right quarter of Fig. 1. The epsilon negative (ENG) material is presented in the top-left quarter, which depicts a negative ε at some frequency regimes and positive μ at all frequencies. This type of material can be achieved by periodic wire structures [62]. The mu-negative (MNG) material is presented in the bottom-right quarter. This material is realized by means of a periodic structure of split-ring resonators (SRRs) [6]. The bottom-left quarter is the most interesting one, in which ε and μ are simultaneously negative, known as double negative materials (DNG). No such material can be found in nature. It can be stated that there are three classes of MTMs depending on the signs of their ε and μ: ENG, MNG, and DNG. The origin of Fig. 1 is classified as zero-index material (ZIM), where ε and μ are at zero. As mentioned earlier, the material with simultaneously $\varepsilon < 0$ and $\mu < 0$ possesses many unique properties. Let us consider a plane wave propagating in a homogenous medium, and its electric and magnetic components are defined as $\vec{E}\left(\omega, \vec{k}\right) = \vec{E}_0\exp\left(\mathrm{i}\vec{k}.\vec{r} - i\omega.\mathrm{t}\right)$ and $\vec{H}\left(\omega, \vec{k}\right) = \vec{H}_0\exp\left(\mathrm{i}\vec{k}.\vec{r} - i\omega.\mathrm{t}\right)$, respectively. Here ω and $\vec{k}$ are the angular frequency and wave vector. Maxwell's equations with no free charges (ρ) and currents ($\vec{J}$) are expressed as follows [63]:

$$\begin{aligned} \nabla\cdot\vec{B} = 0, \quad \nabla\times\vec{E} = \frac{\partial\vec{B}}{\partial t} \\ \nabla\cdot\vec{D} = \rho, \quad \nabla\times\vec{H} = \vec{J} - \frac{\partial\vec{D}}{\partial t} \end{aligned} \tag{3}$$

The constitutive equations are given by

$$\begin{cases} \vec{D} = \varepsilon\vec{E} = \varepsilon_0\varepsilon_r\vec{E} \\ \vec{B} = \mu\vec{H} = \mu_0\mu_r\vec{H} \end{cases} \tag{4}$$

and can be simplified as follows:

$$\begin{cases} \vec{k}\times\vec{E} = \mu\omega\vec{H} \\ \vec{k}\times\vec{H} = \varepsilon\omega\vec{E} \end{cases} \tag{5}$$

where $\vec{D}$ and $\vec{B}$ are the electric and magnetic inductions, respectively. $\varepsilon_0(\mu_0)$ is the free space permittivity (permeability), and $\varepsilon_r(\mu_r)$ is the relative permittivity (permeability) of a medium. From (5), the $\vec{E}, \vec{H}$ and $\vec{k}$ form a right-handed triplet of vectors when the plane wave propagates in positive ε and μ materials, while they form a left-handed triplet in negative ε and μ materials. Furthermore, the Poynting power, $\vec{S} = 0.5(\vec{E}\times\vec{H}^*)$, is used to assess the characteristics of materials and here it is antiparallel to the wave vector $\vec{k}$ in such materials [57]. Due to the above mentioned extraordinary characteristics, materials with $\varepsilon < 0$ and $\mu < 0$ are called left-handed materials (LHMs) or MTM. LHMs support backward-wave propagation, where the phase velocity and group velocity are antiparallel. The electromagnetic wave interacts with the four materials, as shown in Fig. 1. The principle of Snell's law is used to explain the propagation in materials, which is expressed as follows:

$$\frac{sin\theta i}{sin\theta r} = \frac{n_r}{n_i}, \tag{6}$$

where $n_i(\theta_i)$ and $n_r(\theta_r)$ are the refractive indices (angles) of the incident and refraction rays. A positive θ_r can be obtained when both n_i and n_r are positive. Thus, the electromagnetic wave is normally refracted for DPS materials [top-right quarter of Fig. 1]. On the other hand, θ_r is indeed negative when n_i and n_r are positive and negative, respectively, as depicted in the bottom-left quarter of Fig. 1. In other words, the refracted wave bends negatively at the interface. The electromagnetic wave does not propagate in the MNG and ENG materials.

III. MTM INTEGRATION WITH PLANAR ANTENNAS FOR GAIN ENHANCEMENT

The gain is one of the most important performance figures of antennas. In some applications, such as fixed point-to-point communications and radar systems, high gain antennas are instrumental as they are able to enhance the communication range and mitigate interference. It is known that the gain is proportional to the aperture of the antenna, therefore, high profile antennas and array antennas are the most common methods to obtain higher gain. On the other hand, compact antennas are in high demand due to their small size. However, the gain performance of such antennas prohibits their use in many applications where high gain is needed. Clearly, design of compact high-gain antennas is a challenging task. MTMs have been proposed during the last two decades as a low-cost approach for gain improvement without a significant increase of the antenna profile. These artificial materials are placed close to the radiating elements, or etched in the same substrate to manipulate the radiation pattern. A detailed review of different gain enhancement approaches based on MTMs is conducted in this section. As mentioned earlier, the index

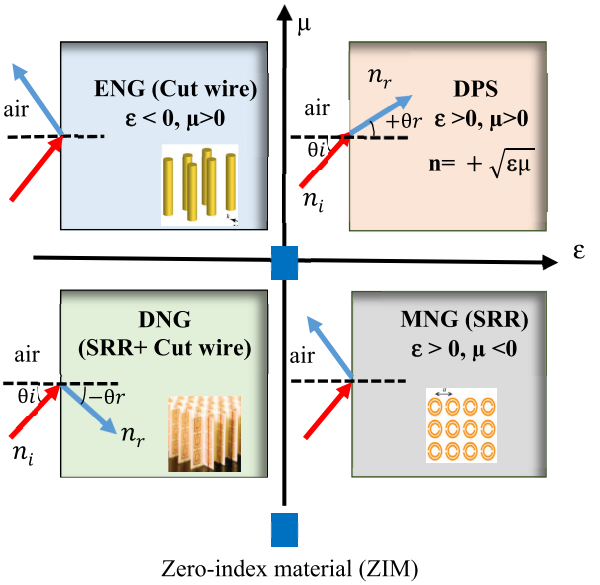

FIGURE 1. Classifications of the materials based on permittivity and permeability with the electromagnetic wave interacting with four possible materials.

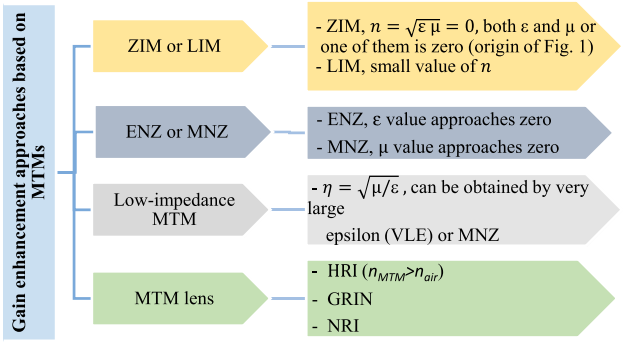

FIGURE 2. The antenna gain enhancement approaches based on MTMs.

of refraction of the material could be positive, zero, or negative. Many research groups had experimentally validated low and zero-index materials (LIMs and ZIMs) [64], [65]. These properties were exploited over the last two decades to improve the performance of planar antennas. Based on Snell's law, these features offered a unique approach for controlling the direction of emission. When either ε or μ (or both) are zero, the ZIM can be obtained. The ENZ or MNZ are also used to control emission direction, thereby improving the gain performance of antennas [66], [67]. On the other hand, the low-impedance property of MTMs is another approach proposed recently for the same purpose [68]. The intrinsic impedance is computed by taking the square root of μ/ε. Therefore, very large epsilon (VLE) $\varepsilon \gg 1$ or MNZ, $\mu \approx 0$, are employed to achieve low-impedance property $\eta_r \ll 1$. This feature can lead to miniaturization of the antenna system by eliminating the air gap between the antenna and the MTM layer [69]. The MTMs serve as meta-lens arranged in layers placed in front/above the radiating part, or etched on the substrate to focus the radiated beam from the planar antenna into the emission direction [70]. The lensing property is based on the high refractive index (HRI) (the MTM refractive index is larger than that of the air, $n_{MTM} > n_{air}$), gradient refractive index (GRIN), and negative refractive index (NRI) materials. In this method, the E-field exhibits the lensing property where MTM slabs convert the spherical waves into the planar ones. Figure 2 shows a classification of the antenna gain enhancement approaches based on MTMs and their properties.

A. GAIN IMPROVEMENT BASED ON ZIM/LIM

In the light of the considerations above, the MTMs are incorporated into the antenna system for enhancing gain and directivity. In the literature, specific characteristics of MTMs such as ZIMs, LIMs, and near zero-index materials (NZIMs) were utilized to achieve this effect. These types of MTMs are widely employed as a beam-focusing material to control the direction of emissions. Pendry *et al.* showed [4], [62] theoretically and experimentally that a plasma frequency characterizes the periodic thin wires, $\varepsilon = 1 - \omega_{p/\omega}$ where $\omega_p(\omega)$ is the plasma frequency (operating frequency). Therefore, the refractive index, $n_{=}\sqrt{\varepsilon\mu}$, approaches zero when the operating frequency approaches the plasma frequency. The gain enhancement capitalizes on the Snell's law of refraction. Here, when the rays of incident angle θi travel from zero-index medium ($n_i = 0$) to air with a high index of refraction ($n_i = 1$), the refracted rays will spread in a direction normal to the interface [71], [72]. Therefore, the phase change of the electromagnetic wave approaches zero or equals zero, thereby inducing a gain enhancement. This is illustrated in Fig. 3, in which the electromagnetic rays pass from ZIM to air in a direction very close to the normal. These interesting characteristics (ZIMs, LIMs, or NZIMs) can be translated into a gain improvement when embedded within antennas. They also motivated many research groups to explore their feasibility to increase the effective aperture of antennas. ZIMs and LIMs (or NZIMs) were used to improve the gain of wide range of planar antennas such as patch antenna [53], [73]–[77], Vivaldi antenna [78]–[81], antipodal tapered slot antenna [82], [83], slot antenna [84], [85], bow-tie antenna [86], quasi-yagi antenna [87], and horn antenna [88].

Microstrip patch antennas exhibit remarkable physical features, such as uncomplicated and low profile structure, as well as low fabrication cost. However, these structures inherently suffer from low gain and narrow bandwidth. Therefore, the ZIMs or NZIMs were loaded to this type of antennas to compensate for the mentioned disadvantages. The ZIMs and NZIMs are usually arranged above the patch antenna with one or multiple layers to improve the gain performance at the desired frequency in the broadside direction. In many reports, these MTM layers are referred to as the superstrate. A single MTM layer was considered in many reports for achieving a high gain augmentation by optimizing the number of unit

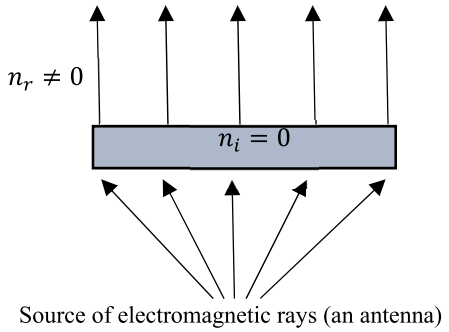

FIGURE 3. A control system for propagation with ZIM layer.

cells and the distance between the antenna and the MTMs. It should be emphasized that including a single layer already increases the overall size of the antenna system, whereas the complexity and size are notably incremented when adding multiple layers. Gain improvement of the patch antenna was achieved by Bakhtiari [73] using NZIM. Only one layer with one unit cell was mounted above the patch antenna at a distance of 20 mm to obtain gain improvement of 8.57 dB at 534MHz. The proposed antenna with one NZIM layer is presented in Fig. 4(a), whereas the gain in E and H-planes are displayed in Figs. 4(b) and (c), respectively. The ZIM-based metallic lines were introduced by Bayat *et al.* to enhance the patch antenna gain [74]. In this report, one layer of the ZIM unit cells was located above the antenna at a distance of 50 mm to enhance its gain by 3.97 dB at 518 MHz. Meanwhile, Ju *et al.* [75] proposed one layer of 7 × 7 ZIMs placed above the feeding patch antenna to improve the gain by 5 dB at 11 GHz. Also, 7 × 7 mirrored S-like unit cells of NZIMs are built as superstrates at a height of $\lambda_0/2$ over the microstrip patch antenna to increase the gain performance by more than 2 dBi at 5.14 GHz [89]. Furthermore, multiple layers of MTMs were mounted over the antenna for further gain enhancement. However, this arrangement leads to an increase in the overall size of the antenna. In [53], Zhou *et al.* proposed splits to the parallel metallic unit cell with ZIM property to enhance the microstrip patch antenna's gain. The MTM structure formed as an array of 4 × 12 unit cells and arranged in two layers above the proposed antenna, cf. Figs. 5(a) and (b). The distance between the antenna and the nearest layer is 16 mm. This arrangement leads to high gain and directivity of 16.2 dB and 17.3 dB, respectively, as illustrated in Fig. 5(c). Li *et al.* proposed electric-field-coupled (ELC) resonator unit cells as ZIM to enhance the patch antenna's gain. The ELC unit cells were arranged in an array of three layers used as a superstrate to accomplish remarkable 7.8 dBi gain improvement at 10 GHz [76]. The unit cell configuration and its refractive index are depicted in Figs. 6(a) and (b); note that the refractive index is very low at 10 GHz. The fabricated prototype of the antenna with three layers of ELC array is demonstrated in Fig. 6(c), whereas the simulated and measured gain is shown in Fig. 6(d).

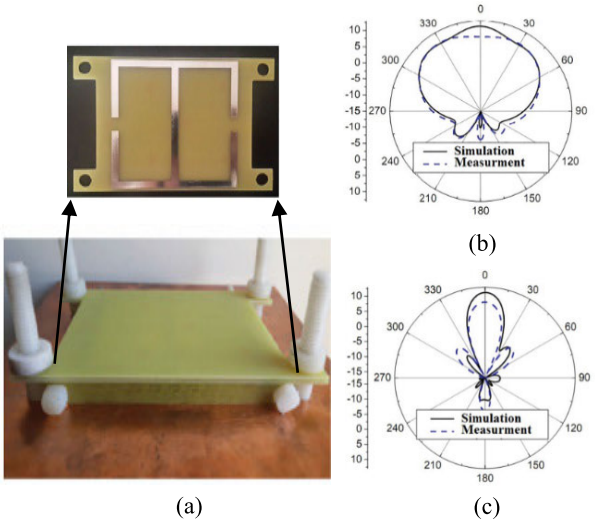

FIGURE 4. The patch antenna of [73] with one layer of NZIM: (a) the fabricated antenna; inset, the fabricated layer of one unit cell of NZIM, and simulated and measured gain at 534 MHz (b) E-plane (c) H-plane.

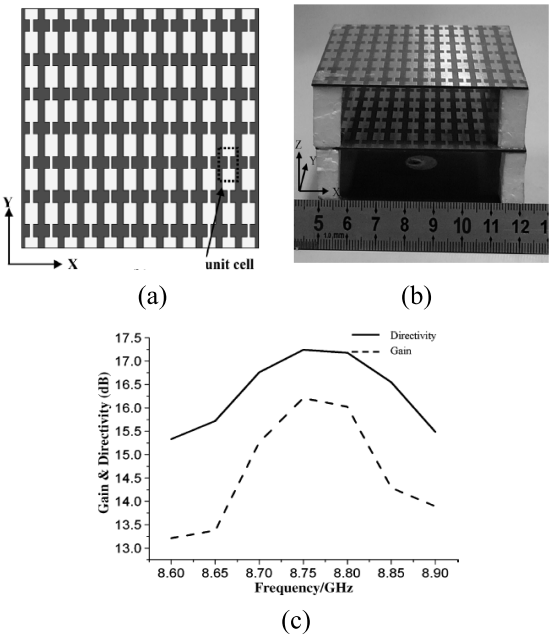

FIGURE 5. MTM antenna based of [53]: (a) the periodic structures of the ZIM, (b) the fabricated prototype, and (c) the measured gain and directivity.

The millimeter-wave band (30–300 GHz) has recently acquired increasing attention due to its advantage of providing higher data rate transmissions. It has been proposed for achieving the 5G multi-gigabit applications [90], [91]. In the 2015 World Radio Communication Conference, the frequency range of 24.25 to 86 GHz had been proposed in the International Mobile Telecommunications for 2020 and beyond [92]. However, these frequencies are affected by high propagation loss due to the short wavelengths, which limits their use for short-range communications. The employment

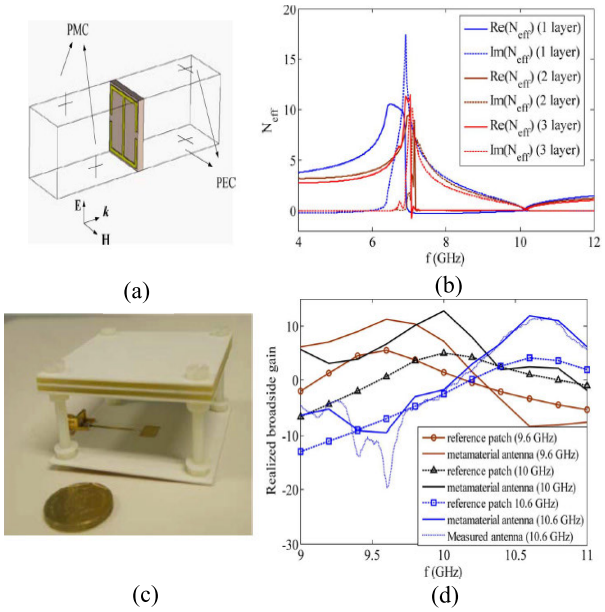

FIGURE 6. The patch antenna with ZIM layers based of [76]: (a) ELC unit cell with boundary conditions setup, (b) the refractive index of the ELC array superstrate, with one, two, and three layer stacking, (c) fabricated prototype of the MTM antenna, and (d) simulated and measured gain of the antenna with and without ELC array.

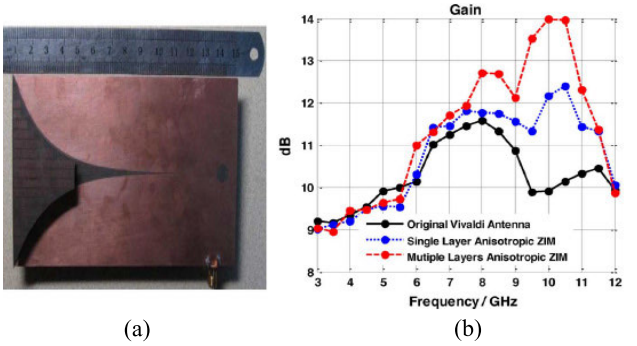

FIGURE 7. Vivaldi MTM antenna based of [78]: (a) fabricated prototype of the antenna with ZIMs, and (b) gain of the antenna with single and multi-layer of ZIMs.

of directional and high-gain antennas is an effective and low-cost approach to increasing the communication range at this band [93]–[95]. Strong candidates to develop high-gain antennas at the millimeter-wave band are MTMs. At this band, MTMs were utilized to enhance the performance of a wide range of single and array antennas, in which some features can be improved with no effect on the antenna size. MTMs help control the antenna array's radiation beam while maintaining the low profile structure [96]. Also, these materials improved the isolation [97], [98], and the isolation and the gain [99] of MIMO antennas. Furthermore, the beam switching and gain enhancement-based MTMs were implemented for single antenna [100] and array antenna [101]. The miniaturization and gain improvement of array antenna based on MTMs were achieved in [102].

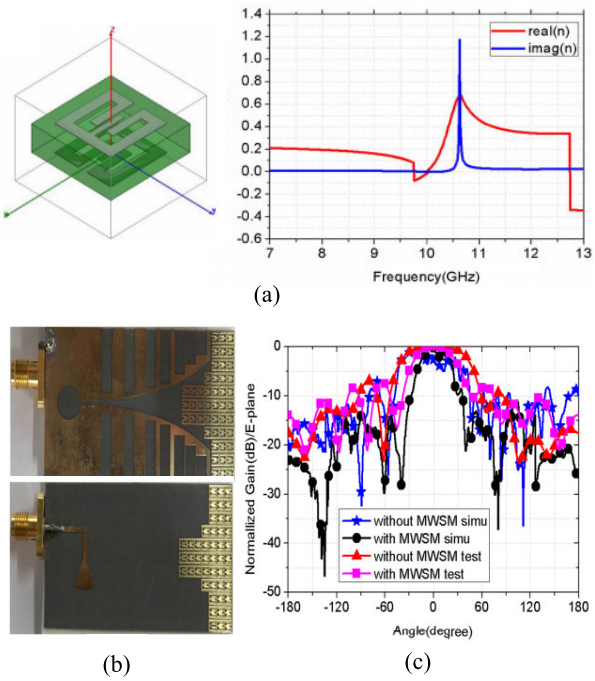

FIGURE 8. The slotted Vivaldi MTM antenna based of [81]: (a) the configuration of the ZIM and its refractive index, (b) the fabricated front and back sides of the Vivaldi antenna loaded by ZIMs, and (c) the simulated and measured normalized gain at 10 GHz.

Gain enhancement at millimeter-wave was proposed by Bouzouad *et al.* [77]. In this report, the gain augmentation was obtained by including single and double layers of NZIMs based Jerusalem cross-unit cells, which were placed vertically above the patch antenna. The gain improvements of 5.1 dB and 7 dB were obtained using single layer and double layers, respectively, over the range of 40-48 GHz. According to the results of this report, increasing the number of layers of the MTMs enables further gain improvements. This is, however, accompanied by the increasing complexity and overall size of the antenna system.

The Vivaldi antenna was studied to attain high gain when loaded with MTMs. Meander-line unit cells with anisotropic zero-index material (AZIM) were used in [78]–[80] for gain enhancement of this type of antennas. The AZIM differs from isotropic (ZIM) by assuming a zero value for only one of the constitutive parameters, either ε or μ, at the desired frequency. This type of MTMs had been proposed theoretically and validated experimentally in [103] and [104], respectively. AZIM has a high capability to transmit and receive electromagnetic waves because of the excellent impedance matching [78]. Moreover, it can enhance radiation efficiency. However, due to their resonant nature, the bandwidth of both ZIM and AZIM is narrow. The meander-line structure has been demonstrated to improve gain of the Vivaldi antenna by 4.07 dB at 10 GHz, 3 dB over 9.5-12.5 GHz, and 2.6 dBi above 5 GHz in [78], [79], and [80], respectively. In these designs, the MTMs were placed in the aperture to focus the

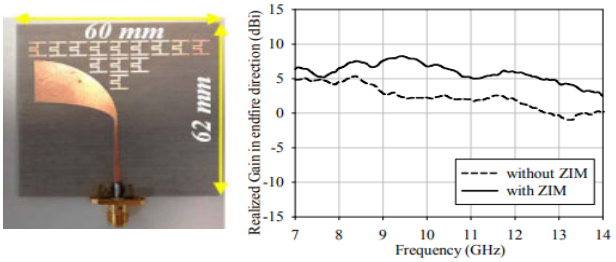

FIGURE 9. ATSA with ZIMs based of [83]: (a) fabricated antenna with ZIMs distributed in the aperture, and (b) the gain with and without ZIM.

electromagnetic waves from the antenna to the direction of emission. Figures 7(a) and (b) show the fabricated prototype of the antenna with ZIM unit cells and the antenna's gain with single- and multi-layer of ZIMs [78]. In [81], modified w-shape metamaterial (MWSM) have been proposed with zero index property at 10 GHz, as illustrated in Fig. 8(a). The ZIM unit cells were etched on both sides of the slotted Vivaldi antenna's aperture to enhance the gain by 4.02 dB at 10 GHz. Figure 8(b) indicates that this design enables gain enhancement while maintaining a low profile structure. The simulated and measured normalized gain at 10 GHz is illustrated in Fig. 8(c).

The antipodal tapered-slot antenna (ATSA) is another type of planar antennas integrated with ZIMs to improve the gain performance. In [82] and [83], the gain increment by 2.6 dB over 57–66 GHz, and 0.3 to 6 dB over 7–14 GHz was obtained, respectively, using an array of ZIMs arranged in the antenna aperture. Both designs feature low profile due to the inclusion of MTM unit cells into the antenna substrate. Figures 9(a) and (b) present the fabricated ATSA with ZIMs and the realized gain of ATSA with and without the ZIMs, respectively [83]. A high gain slot antenna has been introduced by including ZIM and AZIM superstrates [84], [85]. The periodic end-loaded dipole resonator (ELDR) was proposed by Jiang *et al.* to provide the AZIM property [84]. Four layers of 1×14 AZIMs are arranged vertically on the substrate integrated waveguide (SIW) slot antenna for achieving 7 dB gain enhancement at 5.8 GHz, as depicted in Figs. 10(a) and (b). In [85], only one layer of the 3×3 ring resonators with ZIM property was placed above the slot antenna to obtain 7.4 dB of gain augmentation and high efficiency at 8.59 GHz. The performance of the bow-tie antenna in terms of gain augmentation was can be improved by including MTMs at the millimeter-wave band. Dadgarpour *et al.* [86] used the modified Electric-field-coupled (ELCs) resonator with LIMs and double G-shaped resonators (DGRs) unit cells in the front and the back sides of the tilted bow-tie, respectively, for focusing the radiation in the end-fire direction. The radiators of the antenna are tilted by 30 degree for providing better performance. Figures 11(a) and (b) depict ELC and DGR unit cells' configurations, respectively. The low index behavior of modified ELCs is illustrated in Fig. 11(c), whereas the bow-

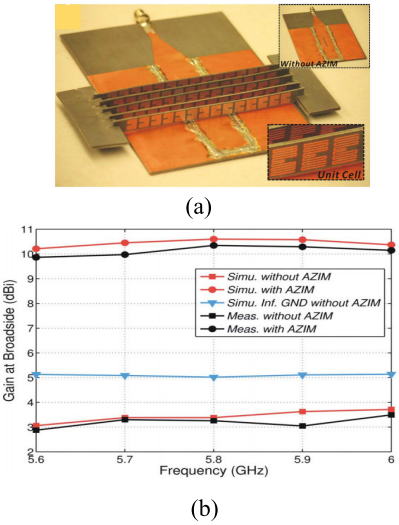

FIGURE 10. SIW slot antenna of [84] with AZIM layers: (a) the fabricated prototype, and (b) simulated and measured gain of the antenna with and without AZIMs.

tie antenna prototype with both MTM structures is shown in Fig. 11(d). The overall gain enhancement is 3.95 dB over 59–64 GHz with a low profile structure, as shown in Fig. 11(e).

The zero-index behavior-based meander line structure was implemented in the front side of two quasi-Yagi antenna arms to enhance the gain by 3.4–5.2 dBi over 1.43–3.9 GHz with a low profile structure [87]. Meng *et al.* [88] combined multi slabs of the metal strips and modified SRR at the antenna's aperture to magnify the gain by 4.02 dB over the frequency range of 8.9–10.8 GHz. The structure is considered bulky due to the arrangement of multi slabs at a distance from the antenna's aperture. Alibakhshi-Kenari *et al.* [105] proposed T- and L-monopole antennas loaded by SRR for enhancing the performance in terms of gain, efficiency, and bandwidth. The measured gains and efficiencies for antennas without SRR loading were 3.6 dBi and 78.5% for F-antenna, and 3.9 dBi and 80.2% for T-antenna at 5 GHz. For antennas with SRR loading, gains and efficiencies were increased to 4 dBi and 81.2% for F-antenna, and 4.4 dBi and 83% for T-antenna.

Table 1 gives the summary of the planar antennas gain enhancement using ZIMs, LIMs, and NZIMs.

B. GAIN IMPROVEMENT BASED ON ENZ/MNZ

The refractive index n is computed based on ε and μ. If the MTM structure has zero or low ε or μ, the resultant refractive index also has zero or low value. Consequently, the mechanism of gain enhancement is based on Snell's law of refraction, as in Section A. Nevertheless, these materials are realized either as featuring near-zero permittivity or permeability, which make the impedance of such materials are not able to match that of the air. This mismatching leads to a significant reduction of the antenna efficiency [88]. The gain enhancement of the patch antenna was performed using ENZ in [66], [106], and MNZ in [107], [67]. A 2.42 dB

TABLE 1. Summary of the antenna gain enhancement using ZIMs, LIMs, or NZIMs.

Ref.	Antenna type	Frequency band	Gain enhancement	Substrate materials	No. of unit cells (No. of layers)	MTM structure (property)
[53]	Microstrip patch antenna	8.75 GHz	-	Rogers 5880, the thickness of 0.787 mm and ε_r of 2.2	4 × 12 (2 layers)	Splits to the parallel metallic slabs (ZIM)
[73]	Patch antenna	534MHz	8.57 dB	FR4, the thickness of 1.6 mm and a ε_r of 4.4	only one unit cell (one layer)	ELC resonators (NZIM)
[74]	Patch antenna	518 MHz	3.97 dB	FR4, the thickness of 1.6 mm and ε_r of 4	7 × 12 (one layer)	Metallic lines (ZIM)
[75]	Rectangular patch antenna	11 GHz	5 dB	Taconic TLY-5, the thickness of 1.57 mm and ε_r of 2.2.	7 × 7 (one layer)	Meandered loops (ZIM)
[89]	Microstrip patch antenna	5.14 GHz	2 dBi	FR4, the thickness of 1.6 mm and ε_r of 4.4	7 × 7 (one layer)	Mirrored S like structure (NZIM)
[76]	Patch antenna	10 GHz.	7.8 dBi	Rogers 4003, the thickness of 0.8 mm and ε_r of 3.55.	30 × 30 (3 layers)	ELC resonators (LIM)
[77]	Patch antenna	40–48 GHz	Max. 7 dB (double layer)	Rogers 5880, the thickness of 0.8 mm and ε_r of 2.2	1 × 7 (two layers)	Jerusalem cross structure (NZIM)
[78]	Vivaldi antenna	10 GHz	4.07 dB	F4B , the thickness of 0.5 mm and εr of 2.65.	Many unit cells distributed on the antenna aperture (4 layers)	Meander-line structure (AZIM)
[79]	Vivaldi antenna	9.5–12.5 GHz	3 dB	F4B , the thickness of 0.5 mm and εr of 2.65.	Several unit cells distributed on the antenna aperture (4 layers)	Meander-line structure (AZIM)
[80]	Vivaldi antenna	5.8–8.5 GHz	Overall 2.6 dBi	FR4, the thickness of 0.8 mm and ε_r of 4.3	16 (-)	Meander-line structure (AZIM)
[81]	Antipodal Vivaldi antenna	10 GHz	4.02 dB	F4B , the thickness of 1 mm and ε_r of 2.65.	47 (-)	MWSM (ZIM)
[82]	Antipodal tapered slot antenna	57–66 GHz.	2.6 dB	Ferro A6S, the thickness of 0.2 mm and ε_r of 5.9	13 (-)	Meander line structure (ZIM)
[83]	Antipodal tapered slot antenna	7–14 GHz	Mas. 6 dB	Rogers RO4003, the thickness of 0.8 mm and ε_r of 3.38	(-)	Meander line structure (ZIM)
[84]	SIW Slot antenna	5.8 GHz	7 dB	Rogers 5880, the thickness of 0.508 mm and ε_r of 2.2	1 × 14 (4 layers)	ELDR (AZIM)
[85]	Slot antenna	8.59 GHz	7.4 dB	R4003C, the thickness of 0.8 mm and εr of 3.38	3 × 3 (one layer)	Ring resonator (ZIM)
[86]	Bow-tie antenna	57–64 GHz	Overall gain enhancement is 3.95 dB	Rogers 5880, the thickness of 0.5 mm and ε_r of 2.2	8 and 2 unit cells etched on both substrate sides (-)	Modified ELC and DGR (ZIM)
[87]	Quasi-Yagi antenna	1.43–3.9 GHz	3.4–5.2 dBi	FR4, the thickness of 1.6 mm and εr of 4.4	1 × 7 (-)	Meander line structure (ZIM)
[88]	Horn antenna	8.9–10.8 GHz	4.02 dB	-	1 × 13 (-)	MSRR (ZIM)

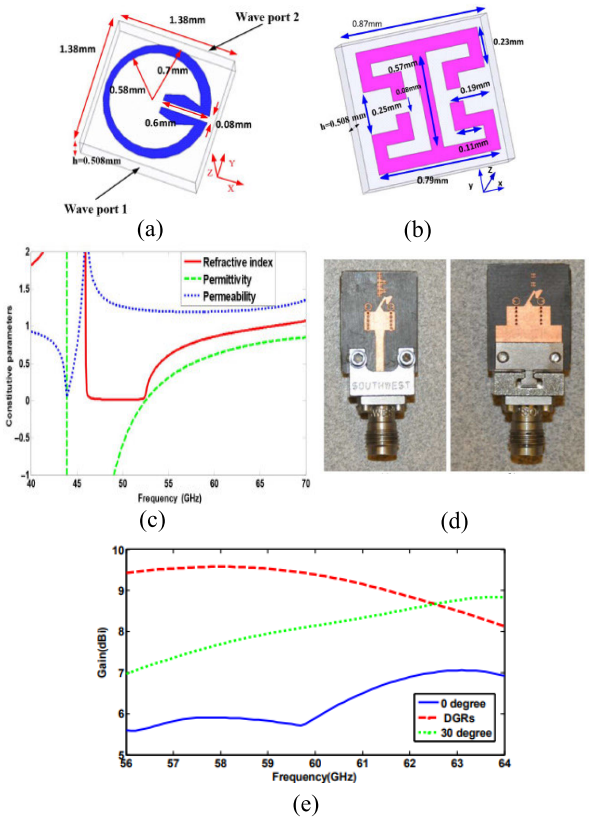

FIGURE 11. Bow tie antenna of [86] with two MTM structures: (a) modified Electric-field-coupled (ELC), (b) double G-shaped resonators (DGR), (c) constitutive parameters of modified ELC structure, (d) the fabricated prototype, and (e) the gain for un-tilted (0 degree) and tilted radiators (30 degree), and the antenna gain for a tilted bow-tie antenna with DGR loading.

of gain enhancement was obtained when multi-layer ENZ arranged above the patch antenna at 1.85 THz, where the principal of Snell's law was used to explain the gain improvement approach [66]. The MTM structure consists of alternating layers of indium antimonide (*InSb*) and silicon dioxide (SiO_2), as illustrated in Fig. 12(a). Figure 12(b) demonstrates the increase of the antenna gain when loaded by the ENZ layers compared to that of the basis structure. Abdelgwad and Said [106] proposed one layer of periodic wire structure with the ENZ property to increase the gain and the bandwidth of a patch antenna with the gain augmented by 4.7 dB at 1 GHz. The conventional SRR structure offers the MNZ property in [107], [67]. Yoon *et al.* [107] presented six plates, each with 4 × 5 SRRs placed above the array of patch antennas for enhancing the gain by 2.75 dBi at 3.2 GHz, as demonstrated in Figs. 13(a) and (b). Further, Gangwar *et al.* [67] discussed the gain enhancement of a patch antenna based on the MNZ superstrate. A gain augmentation of 7.6 dB at 5.9 GHz was obtained by including four layers of MNZ above the patch antenna, as presented in Fig. 14. The size and the complexity of the entire structure are increased due to the inclusion of multi-layer MTMs that form a 3D structure. A high gain Vivaldi antenna was implemented by loading the meandered-line structure exhibiting the ENZ property in [108], [109]. The dual-band gain enhancement was achieved by El-Nady *et al.* at the millimeter-wave spectrum [108]. In this report, 5 × 1 ENZ unit cells were printed in the same substrate of the Vivaldi antenna to enlarge the gain by 5.2 dB at 30 GHz, and by 6 dB at 40 GHz. On the other hand, Pandey *et al.* [109] proposed a compact ENZ based on meandered line unit cells. The ENZ unit cells were incorporated into the aperture of the conventional vivaldi antenna (CVA) resulting in gain enhancement of 2 dBi over the frequency range of 3.1–12 GHz, as demonstrated in Figs. 15(a) and (b). Dadgarpour *et al.* [110] designed seven layers, each with 2 × 7 SRRs having MNZ property, located vertically on the bow-tie antenna's substrate. Gain enhancement of 5–6.5 dBi was obtained over 5.65–7.85 GHz. Table 2 summarises the usage of ENZ and MNZ for gain enhancement of planar antennas.

C. GAIN ENHANCEMENT BASED ON LOW IMPEDANCE MTM

Gain improvement of the magnetic-dipole sources can be achieved by embedding low-impedance MTMs [68]. According to [69], [111], the broadside power density of a magnetic dipole source can be improved using low impedance MTMs arranged in an array form in the near field of the source, which can be supported by the expression of $P_m(0) = (k_o^2/8\pi^2\eta_0\eta_r^2)$, where $P_m(0)$ is the far-field power density (W/sr), $k_0 = 2\pi/\lambda_0$ is the wavenumber, $\eta_0 = 377$ is the free space impedance, and η_r is the intrinsic impedance. Recently, MTM structures with the low-impedance property were used to enhance the gain of planar antennas. As mentioned earlier, MTMs are periodic metallic structures responsible for inducing electric and/or magnetic dipoles by an incident electromagnetic wave. These dipoles alter the effective characteristics of the material. The intrinsic impedance (η) of an MTM is given by $\varepsilon\sqrt{\mu/}$. Thus, VLE or MNZ exhibits a low-impedance property. This allows for reducing the overall size of the antenna system by diminishing the air gap between the antenna and the MTM layer. In these designs, the real part of ε should be sufficiently large to satisfy the condition of $\varepsilon \gg 1$ for a VLE material or the μ should be extremely small for realizing the MNZ material, which finally yields a low impedance material with $\eta \ll 1$. The low impedance MTMs were integrated with slot antennas to enhance the gain performance in [54], [68], [69], [112], [113].

Pandit *et al.* [112] proposed 3 × 3 star shape unit cells placed above the SIW-based slot antenna with a minimal distance of λ/15. The MTM unit cell configuration and its constitutive parameters are shown in Fig. 16(a), which offer a low impedance property around 9.8 GHz. The proposed antenna with MTM is presented in Fig. 16(b). It achieves a gain improvement of 5 dB at 9.8 GHz, as depicted in Fig. 16(c). Pandit *et al.* [68] introduced one layer of 5 × 5 square-ring (SR) unit cells located directly on the slot antenna to enhance its performance. The proposed MTM with low impedance property at 9.78 GHz improves the antenna's gain by 8.3 dB.

TABLE 2. Summary of using ENZ and MNZ for gain enhancement of planar antennas.

Ref	Antenna type	Frequency band	Gain enhancement	Gain enhancement based on	No. of unit cells (No. of layers)	MTM structure
[66]	Patch antenna	1.85 THz	2.42 dB	ENZ	Each layer is one unit cell (11 layers)	Multi-layer of InSb and SiO_2
[67]	Patch antenna	5.9 GHz	7.6 dB	MNZ	4 × 4 (4 layers)	SRR
[106]	Patch antenna	1 GHz	4.7 dB	ENZ	5 × 1 (one layer)	Periodic wire structure
[107]	Patch antenna	3.2 GHz	2.75 dBi	MNZ	4 × 5 (6 layers)	SRR
[108]	Vivaldi antenna	30 and 40 GHz	at 30 GHz (5.2 dB), at 40 GHz (6 dB)	ENZ	5 × 1 (-)	Quasi mender line
[109]	Vivaldi antenna	3.1–12 GHz	2 dBi	ENZ	13 (-)	Compact meandered line
[110]	Bowtie antenna	5.65–7.85 GHz.	5–6.5 dBi	MNZ	2 × 7 (7 layers)	SRR

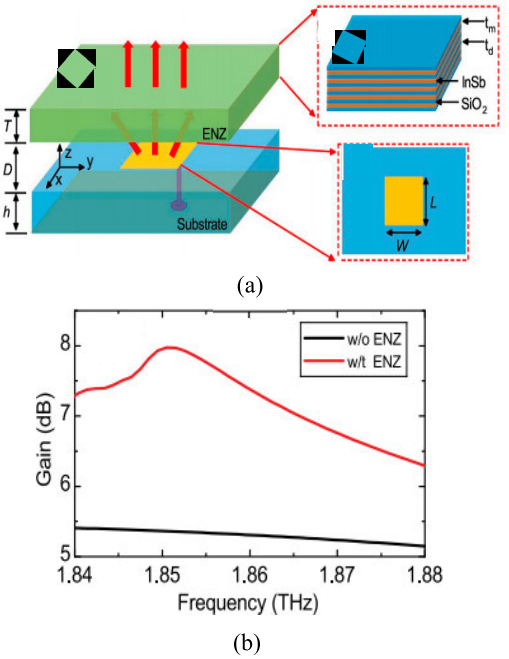

FIGURE 12. Patch antenna with multi-layer of ENZ based of [66]: (a) the configuration MTM antenna, and (b) the antenna gain with and without ENZs.

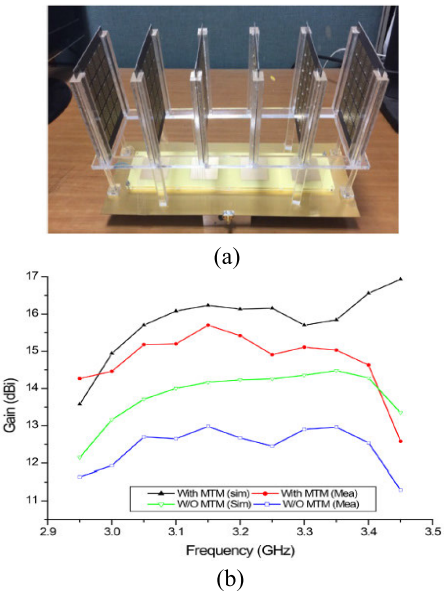

FIGURE 13. Patch antennas array with MNZ layers based of [107]: (a) the fabricated prototype, and (b) simulated and measured gain of the antenna with and without MTM.

Figure 17(a) shows the SR unit cell with its impedance, whereas μ and ε are presented in Fig. 17(b). It can be seen that the value of ε is high in comparison with μ, which leads to a low impedance property of the proposed MTM. Figures 17(c) and (d) depict the fabricated prototype and the gain enhancement in the presence of low impedance MTM. In [69], a single MTM unit cell was installed on the ground of a ring slot antenna (RSA) to obtain a low impedance behavior, thereby enhancing the gain by 5.99 dBi at 1.9 GHz. The ring resonator structure reveals a high ε of 50 and very low μ resulting in a low impedance of 0.1 at 1.9 GHz, as shown in Figs. 18(a) and (b). The fabricated antenna prototype with a single MTM unit cell has been displayed in Fig. 18(c), whereas the antenna gain is displayed in Fig. 18(d). Furthermore, the cross circular loop resonator (CCLR) MTM structure was proposed by Pandit *et al.* in [113] to achieve the low impedance property. Figures 19(a) and (b) present the configuration of the low impedance CCLR unit cell and its constitutive parameters, in which it provides a high value of ε and very low μ. An array of low impedance CCLR unit cells were embedded above the substrate integrated waveguide fed-slot antenna (SIW-SA) to magnify the gain by 5.8 dB at 9.73 GHz, as illustrated in Figs. 19(c) and (d). The VLE property of MTM has been used to improve the gain of the dual-band circularly polarized (CP) antenna for medical applications in [54]. The proposed MTM

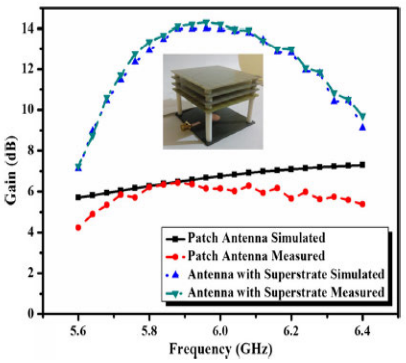

FIGURE 14. Fabricated prototype with simulated and measured gain of the patch antenna with and without MNZ layers [67].

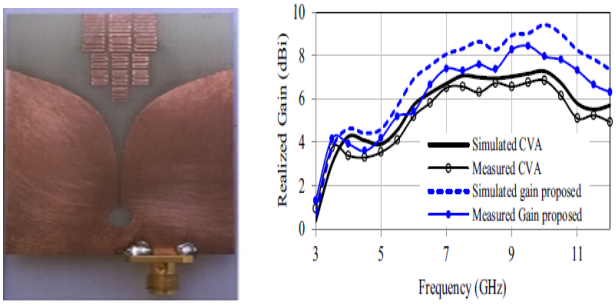

FIGURE 15. CVA with ENZs based of [109]: (a) the MTM antenna prototype, and (b) simulated and measured gain.

antenna achieves a high gain of 17.1 and 9.81 dBi in the lower band of 915 MHz and upper band of 450 MHz, respectively. Furthermore, it realizes a CP operation at both frequencies. Despite the small number of published reports, this approach certainly has a great potential in enabling gain improvement (8.3 dB in [68]) while reducing the overall size and the complexity of the antenna system, the latter ensured through a reduction of the air-gap between the antenna and the MTMs. Such an approach would require more investigation through integration of different MTM shapes with various antennas.

D. GAIN IMPROVEMENT BASED ON LENSING PROPERTY OF MTMS

Lens antennas have gained considerable attention due to their advantages in providing wideband and high-gain performance through focusing the radiation into a narrow beamwidth in the required direction. The dielectric materials are used as traditional lenses [114], [115]. However, they ultimately suffer from the high profile structures as well as complex and expensive fabrication process. As an alternative, artificial materials (e.g. MTMs) are used as lenses, which are integrated with antennas to convert the spherical waves into the planar ones. Various MTM structures act as meta-lens organized in an array form of single or multi-layer, in which they can be etched on the substrate or placed in front/above

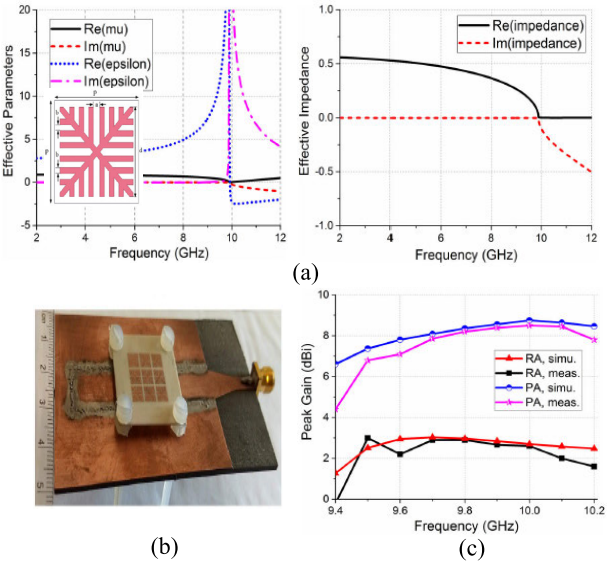

FIGURE 16. SIW slot antenna of [112] with low impedance MTM: (a) the star-shape MTM unit cell and its μ and ε, and, impedance, (b) the fabricated prototype of the MTM antenna, and (c) simulated and measured gain of reference antenna (RA) and proposed antenna (PA) with MTM.

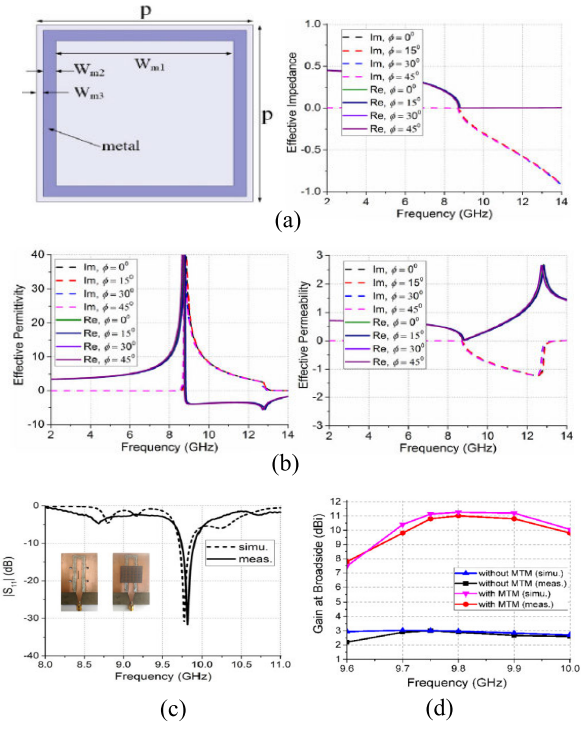

FIGURE 17. Slot antenna with low impedance MTM based of [68]: (a) the SR unit cell and its impedance, (b) the real and imaginary parts of the μ and ε, (c) reflection coefficient and fabricated prototype of the MTM antenna, and (d) simulated and measured gain.

the antenna's radiating part. Unlike traditional curve lenses, the MTM lens is designed using an utterly planar structure, which leads to a considerable enhancement of the antenna gain based on the different characteristics of the refractive

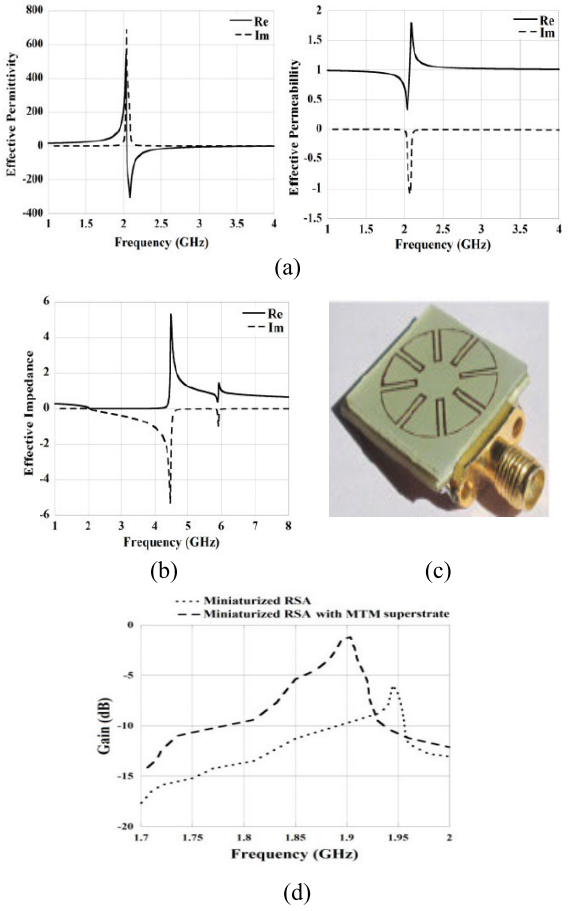

FIGURE 18. RSA with low impedance MTM based of [69]: (a),(b) the real and imaginary parts of the μ and ε, and, impedance of the ring resonator, (c) photograph of fabricated prototype of the antenna with single MTM unit cell, and (d) the antenna gain with and without MTM.

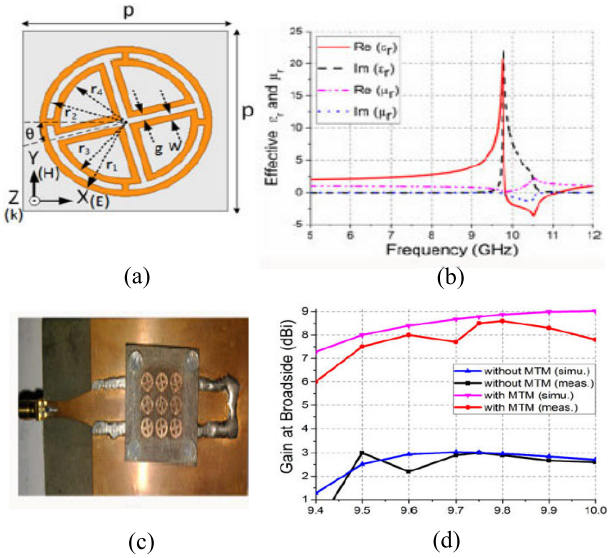

FIGURE 19. SIW-SA with low impedance MTM based of [113]: (a), (b) CCLR structure and its constitutive parameters; ε and μ, (c) photograph of the fabricated MTM antenna, and (d) simulated and measured gain of the antenna with and without low impedance MTM.

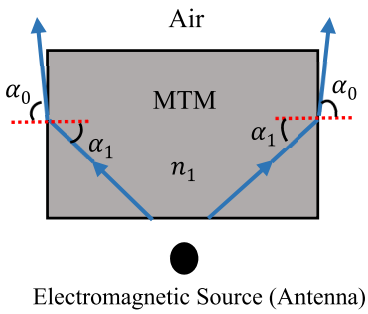

FIGURE 20. Mechanism of gain enhancement based on HRI approach.

index. The unique properties of the MTMs can manipulate the propagation of electromagnetic waves resulting in the freedom to design different types of lenses such as the high refractive index (HRI) lens ($n_{MTM} > n_{air}$), GRIN, and NRI.

1) MTM LENS BASED ON HRI

In this subsection, MTM Lens is exhibited based on HRI. MTMs with a refractive index higher than that of the air ($n_{MTM} > n_{air}$) act as meta-lens to focus the radiation on the direction of emission where the beam can aggregate in the end-fire direction. The principle of refractive index law can explain the mechanism of gain enhancement. Figure 20 shows the wave propagation in both mediums; MTM and air. From the Snell's law, when the incident angle α_1 is fixed, the high value of the refractive index leads to a larger refractive angle α_0.

To achieve such a property, the refractive index of the proposed MTM layer should be larger than 1 ($n > 1$) at the desired frequency. Thus, the energy passing through the MTM structure is converged and focused in the direction of emission. The E-field is utilized to show the lensing property where MTM slabs convert the spherical waves into the planar waves and reduce the half-power beamwidth (HPBW). To implement this approach, different MTM structures are integrated with various planar antennas [116]–[123]. Chen *et al.* [116] introduced parallel lines unit cells embedded into the aperture of the antipodal tapered slot antenna (ATSA), as illustrated in Fig. 21(a). These unit cells acted as a conventional lens for beam focusing where the gain was improved by 1.3–3.6 dB over the range of 6–19 GHz. The gain enhancement and the retrieved refractive index are displayed in Figs. 21(b) and (c), respectively. The principle of the refraction law explained in Fig. 20 is applied here. From Fig. 21(c), the refractive index of the considered unit cell is larger than 1 ($n > 1$) below 19 GHz. Thus, the energy transferred through the MTM structure is converged, thereby improving the antenna gain. The same mechanism was also applied in [117]–[123]. In the first three reports, an array of I-shape resonator (ISR) was incorporated in the same substrate of the end-fire antennas for gain enhancement purpose. The

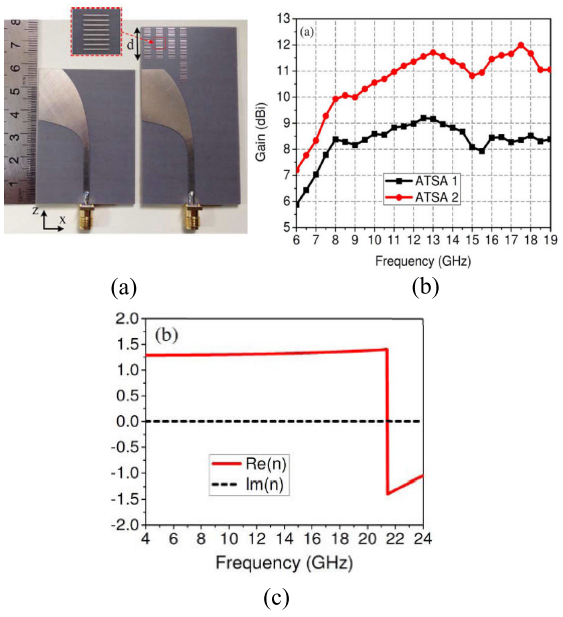

FIGURE 21. ATSA with HRIs based of [116]: (a) the fabricated antipodal tapered slot antenna (ATSA) with parallel lines lens, (b) measured gain of antenna alone (ATSA1) and antenna with MTM lens (ATSA2), and (c) refractive index of considered unit cell.

gain of bow-tie end-fire antenna is promoted by 1.5–3.5 dB over 5.1–8.3 GHz with a reduction in the side lob level [117]. In parallel, gain enhancements of 2–3.5 dB over 3–11 GHz and 2 dB over 4.5–9.5 GHz were achieved for periodic end-fire antenna and quasi-Yagi antenna in [118] and [119], respectively. Wang *et al.* [120] presented 2 × 5 H-shaped resonator (HSR) unit cells to boost bow-tie gain. The HSRs were etched into the substrate to achieve 0.5–6.0 dB gain enhancement over 2.31–3.93 GHz. The non-resonant MTMs are commonly obtained by simple designs, such as metal thin circular rings and metal blocking lines, which are usually used to enhance antenna performance and reduce the inherent loss of MTM [124]. Zhai *et al.* [121] proposed a non-resonant MTM for improving the gain of log-periodic dipole array fed by SIW operating at millimeter-wave band (26–40GHz). In this report, three cases 1, 2, and 4a were studied to show the gain enhancement, as depicted in Fig. 22(a). A maximum gain improvement of 4 dB was obtained at 27 GHz with enhancing antenna efficiency, as depicted in Fig. 22(b). The gain of the dipole and bow-tie antennas was improved by 5 dB over 26–30 GHz and 2 dB over 5–11 GHz in [122] and [123], respectively. Six slabs of 3 × 3 of two-sided planar metamaterial (TSPM) unit cells were proposed by Khajeh-Khalili *et al.* to magnify the bow-tie antenna gain [70]. These slabs worked as a lens embedded vertically onto the azimuth plane, in which the interactions between them increase the antenna's aperture size, thereby improving antenna gain. Figures 23(a) and (b) demonstrate the fabricated MTM lens with a bow-tie antenna and the realized gain with different MTM lens layers. As can be seen, the gain enhances as the MTM lens layers increase.

2) GRIN LENS BASED ON MTM

GRIN lenses have attracted considerable attention owing to their ability to focus the radiation. These lenses have been proposed as alternatives to the established dielectric ones, where the refractive index is different throughout the lens rather than being dependent on the interfaces of the dielectric material to manipulate and shape the radiation beam. Among the most known lenses are Luneburg and Maxwell fisheye; the gradient refractive index distribution of the former is expressed by $n_r = \sqrt{2-(r/R)^2}$, whereas the distribution of the latter is given by $n_r = n_0/1+(r/R)^2$ [125], [126]. In both formulas, R and r are the lens radius and the distance from any point to the lens centre, respectively. Both lenses have the capability to focus a point on their surfaces to the diametrically opposite side. Achieving GRIN with the proper refractive index distribution is the main concern as they are artificial materials and need different ways to be synthesized. Alternatively, the distribution of the refractive index can be realized based on MTMs, where it is achieved by geometric tailoring of the neighbouring unit cells [127]. The homogeneous MTMs can be achieved by identical unit cells arranged in an array form, which are used in a wide range of applications. On the other hand, if the unit cells are not identical, the inhomogeneous medium, here the GRIN, can be realized. The inherently non-resonant, wide bandwidth, and low-loss behaviour of GRIN based MTMs enable many practical applications, such as the realization of the various lenses to enhance the performance of antennas in terms of the high gain and directivity, efficiency, beam deflection, low sidelobe, and broad bandwidth [128]–[133]. The idea of utilizing GRIN to manipulate the propagation of electromagnetic waves was introduced by Smith *et al.* in [134], where the SRR was used to tilt the microwave beam. This medium acts as meta-lens to transform the spherical waves to the planar ones, thereby enhancing the antenna gain and directivity. Nevertheless, such inhomogeneous mediums require time-consuming design process, and, in most cases, they are highly polarization-sensitive [133], [135]. A variety of GRIN lenses were proposed in the literature for enhancing the gain performance [115], [136]–[139]. Seven layers of GRIN lenses were set in front of the tapered slot antenna (TSA) for increasing the gain by 6 dB at 10 GHz, as shown in Figs. 24(a) and (b) [136]. The nonresonant parallel-lines metallic strips are used to build the GRIN lens. The gain enhancement mechanism is based on the lensing property of GRIN MTM, and this feature can be explained by the E-field distribution of the TSA and TSA with GRIN MTM at 10.5 GHz [Fig. 24(c)]. It can be seen that the field of TSA with GRIN MTM is stronger compared to that of TSA alone, which supports the lensing property of GRIN MTM and transfers the spherical waves into the planar ones.

In a more complex way, Xu *et al.* [137] proposed several 3D GRIN lenses for enhancing the monopole antenna performance in terms of gain and beam steering. These lenses were installed circularly around the antenna to focus the

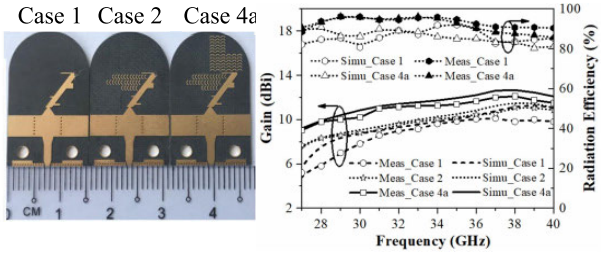

FIGURE 22. The log-periodic dipole array fed by SIW with non-resonant MTM based of [121]: (a) the photograph of the antenna with and without non-resonant semi-ring unit cells, and (b) the simulated and measured gain and efficiency.

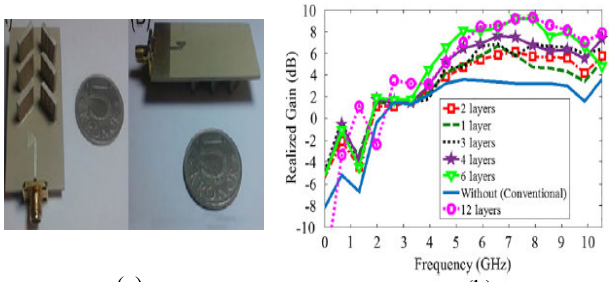

FIGURE 23. Bow-tie antenna of [70] with MTM lens: (a) front and back views of the fabricated MTM antenna, and (b) realized gain with different layers of TSPM unit cells.

radiation resulting in a maximum gain increment of 10 dB over 3–8 GHz, as illustrated in Figs. 25(a) and (b). The quasi-spherical waves were successfully transformed into the plane waves by comparing the wavefronts of the lens antenna and monopole alone, cf. Fig. 25(c). Besides the high gain, this antenna system exhibits the advantages of broadband operation and beam deflection. The ATSA integrated with GRIN rectangular rings for magnifying the gain by about 9.5 dB over 7–12 GHz [115]. The GRIN lens here consists of strips of different sizes that exhibit different refractive index in the range of 1.2 to 3.7. This arrangement enhances the efficiency and reduces the side lobe level. The authors of [139] proposed GRIN lens layers that are placed above the Vivaldi antenna for focusing the electromagnetic wave and enhancing the gain by about 4 dB over 10.5–12.5 GHz. The complementary non-resonant closed ring (CCR) unit cells were used to achieve a gradient refractive index profile. Here, the refractive index distribution is based on the conventional half Maxwell fish-eye lens.

3) MTM LENS BASED ON NRI

The NRI is another type of beam focusing lens, in which these materials act as a convergent planar lens used for focusing electromagnetic waves, thereby enhancing the gain performance of antennas. In the literature, different MTM structures exhibiting negative refraction property used to enhance the performance of several antennas at different

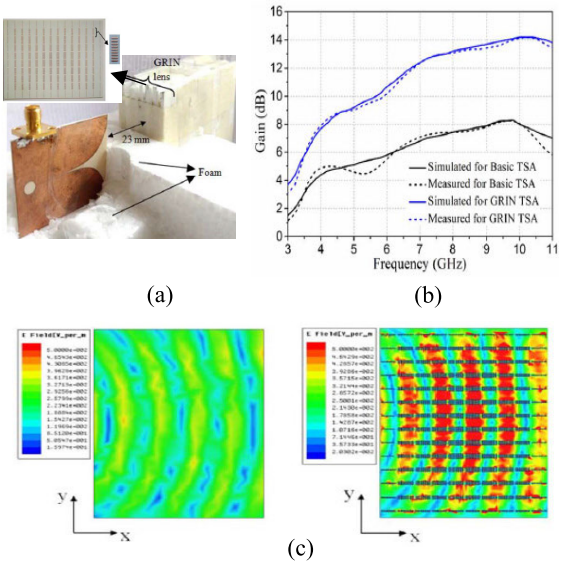

FIGURE 24. TSA with GRIN lens based of [136]: (a) the fabricated antenna with seven GRIN MTM lenses, (b) the simulated and measured gain, and (c) simulated the E-field distribution of the TSA and TSA with GRIN MTM at 10.5 GHz.

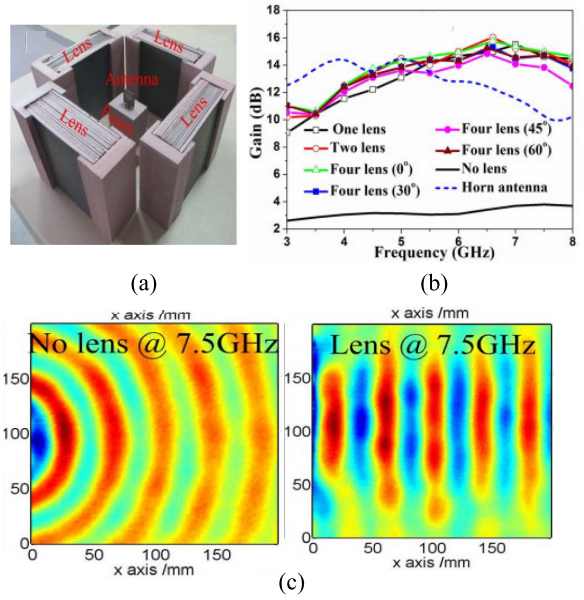

FIGURE 25. Monopole antenna of [137] with MTM lenses: (a) the fabricated four MTM lenses with antenna, (b) the gain with multi-layer and angles rotation of MTM lens, and (c) measured electric-field of the antenna with and without lens at 7.5 GHz.

frequency bands [140]–[154]. The performance of the dielectric resonator antenna (DRA) was boosted using the MTM lens in [140], [141]. A single layer of 4 × 4 E-shaped resonator (ESR) unit cells is placed over the slot-coupled hemispherical DRA for amplifying the gain with a better reflection coefficient and reduced HPBW in both the H- and E-planes [140]. Figure 26(a) shows the reflection coefficient and prototype of the proposed MTM antenna. The MTM array acts as a lens to focus the waves, thereby enhancing the

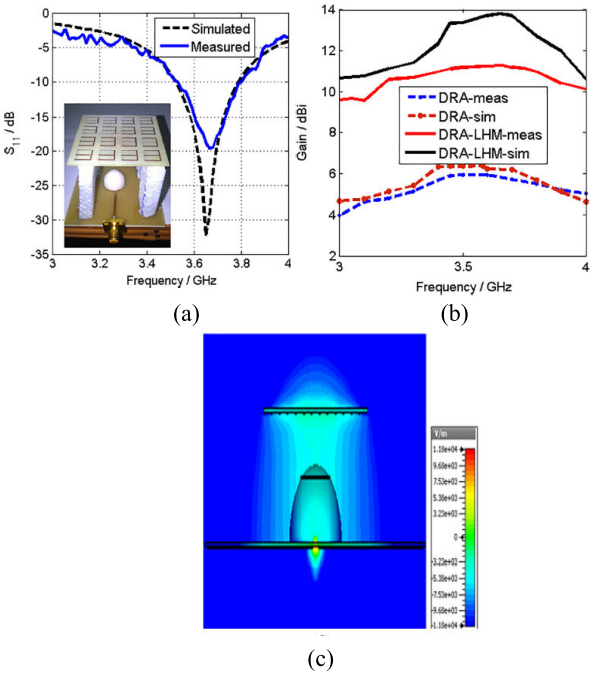

FIGURE 26. DAR with NRI lens based of [140]: (a) reflection coefficient and prototype of antenna with MTM lens, (b) simulated and measured gain with and without of MTM lens, and (c) simulated E-field of the antenna with MTM lens at 3.65 GHz.

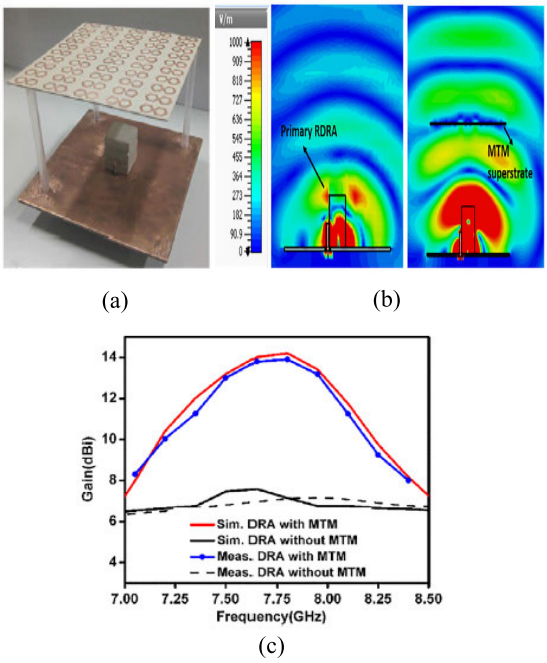

FIGURE 27. DAR with MTM lens based of [141]: (a) the fabricated prototype, (b) the simulated E-field of the antenna with and without MTM lens at 7.5 GHz, and (c) simulated and measured gain.

gain by 6 dB at 3.65 GHz, as shown in Fig. 26(b). Figure 26(c) presents the E-field at 3.65 GHz to show the lensing property where MTM slabs convert the spherical waves into the planar

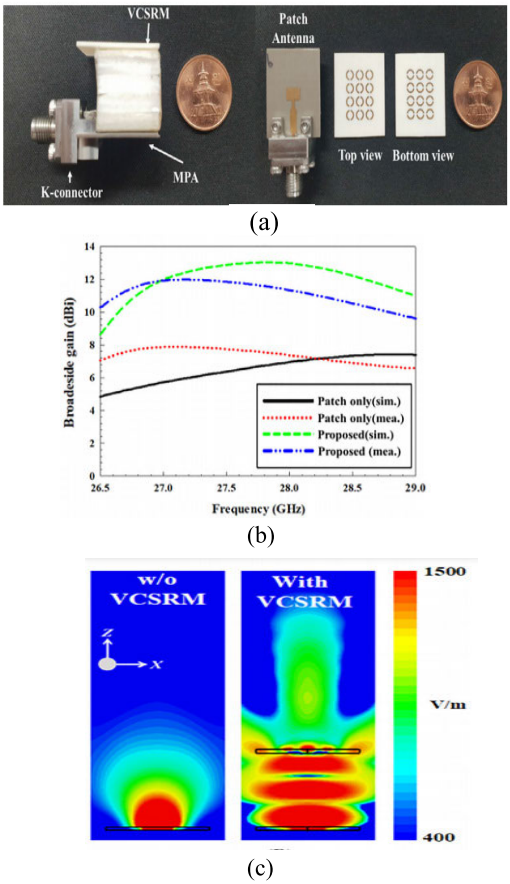

FIGURE 28. Patch antenna with MTM lens based of [143]: (a) the photograph of the fabricated MTM antenna, (b) the simulated and measured gain of the proposed antenna alone and in the presence of VCSRMs, and (c) simulated electric-field of the antenna with and without MTM lens at 28 GHz.

ones. Pandey *et al.* [141] proposed a single layer of 5 × 10 infinity shape resonator (ISR) unit cells to increase the rectangular DRA's gain by 6.5 dB at 7.8 GHz. Figure 27(a) shows the photograph of the fabricated rectangular DRA with the MTM lens layer. The electric field of the antenna with and without ISRs were studied at 7.5 GHz, as depicted in Fig. 27(b). For the bare DRA, the field is concentrated near the antenna only and degraded at the far-field. On the other hand, the electric field is strengthened in the far-field when the antenna is loaded by ISRs. Figure 27(c) demonstrates that the gain enhancement is noticeable when the MTM lens is loaded.

Alhawari *et al.* [142] used seven layers, each with 3 × 4 unit cells in front of the Vivaldi antenna to focus the radiation. These layers were arranged vertically between the two arms of the proposed antenna for improving the gain by 4 dB over 6.5–20 GHz. The gain performance of the microstrip patch antenna (MPA) is enhanced based on the MTM lens in broadside direction [143]–[152]. The performance of the MPA is enhanced in terms of gain and bandwidth in [143]–[146]. In [143], Jeong *et al.* introduced the

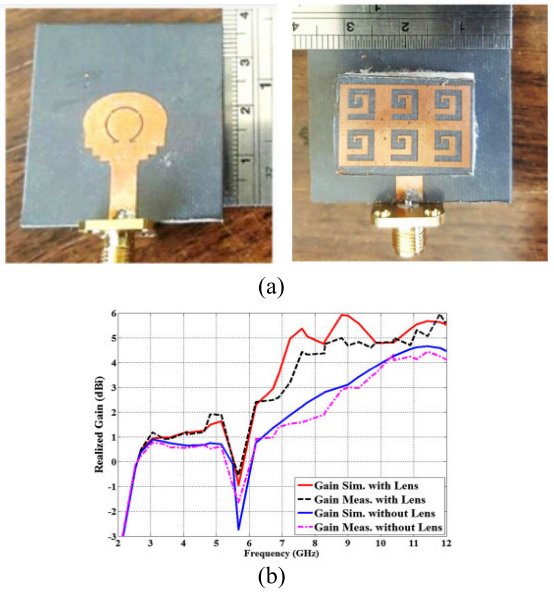

FIGURE 29. UWB antenna of [153] with MTM lens: (a) the fabricated prototype, and (d) simulated and measured gain of the antenna alone and antenna with lens.

vertically coupled split ring metaplate (VCSRM) unit cells arranged in one layer lens over the MPA at millimeter-wave spectrum (26.58 to 29.31 GHz). The antenna lens is illustrated in Fig. 28(a). This arrangement results in focusing the radiation in a broadside direction and enhancing the gain by 5.35 dB (maximum), as depicted in Figs. 28(b) and (c). Furthermore, the bandwidth is improved by 3.9%. In [144] and [146], the conventional SRR and cut wire unit cells were used to focus the radiation, and broaden the bandwidth of the array MPA at the microwave spectrum. The array antenna spherical waves enter the lens and convert to the planar ones at its output. In addition, the performance of MPA was enhanced in terms of the gain [147], gain and size [148], gain and efficiency [149], and gain and isolation [150]. Gupta *et al.* [151] used the square Minkowski fractal-shaped MTM for focusing the radiation and enhancing MPA gain by 2.9 dB at 11.4 GHz. A single-layer of modified square SRR unit cells was added to the corner of the dual-band MPA to enhance the gain by 3.69 dB at the lower band of 2.5 GHz [152]. Ali *et al.* [153] proposed an array of inverted L-shaped MTM to operate as a lens placed in the near field of UWB antenna, as illustrated in Fig. 29(a). The negative value of ε enhanced the electric fields in the near region of the antenna, thereby enhancing the proposed antenna's gain and directivity. Figure 29(b) shows that the gain improvement at the operating frequencies is more than 2.5 dB. The MTM lens is etched in the same substrate of the quasi-Yagi antenna for promoting the gain by 4.71 dBi at 3.8 GHz [154]. The loaded MTM with a refractive index lower than that of the substrate helps to achieve gain and directivity enhancement. It also assists in enhancing the bandwidth and provides a compact lens size.

The composite right–left-handed MTM transmission-lines were utilized to enhance the gain and other features of the antenna [155]–[157]. The L/F-shaped slits and spirals for establishing a series-capacitor and shunt-inductor effects, respectively, were used to enhance the properties of the planar antenna [155]. With cascading the proper number of the MTM unit cells, the desired properties of the antenna were achieved. By including four L-shaped cells, the antenna provided a bandwidth of 0.2–1.8 GHz with the highest gain and efficiency of 3.4 dBi and 88% at 1550 MHz, respectively. The antenna performance was improved by embedding five F-shaped unit cells, where the maximum gain and efficiency were 4.5 dBi and 95% at 1900 MHz, respectively. In the same way, the L-shaped slits with inductive spiral unit cells were loaded to the rectangular radiating patch for enhancing the radiation characteristics and bandwidth. Increasing the number of unit cells was crucial for superior performance with a minimal effect on the antenna size [156]. By including four unit cells, the MTM antenna provided bandwidth, gain, and efficiency of 6.15 GHz, 3.68 dBi, and 73.4%, respectively, at 3.25 GHz. When increasing the spiral turns, the gain and efficiency were slightly improved to 3.83 dBi and 73.7%, respectively. The performance of the rectangular patch antenna was improved by embedding a complementary artificial magnetic conductor MTM structure [157]. E-shaped slits and inductive microstrip lines realized MTM unit cell. Three antennas were studied by increasing the number of MTM unit cells for better performance. The best performance was obtained by including two rows of five unit cells above the patch antenna, where the maximum gain and efficiency were 4.45 dBi and 85.8% at 2.76 GHz, respectively. Moreover, it provided a high bandwidth of 3.69 GHz.

Table 3 provides the summary of gain improvement of planar antennas using the MTM lens.

The review carried out in this work allows us for several observations concerning the design and realization of gain-enhanced antennas based on MTMs. The following key aspects should be emphasized:

- There exist many approaches to realize gain enhancement of antennas, such as the arrangement of the planar antennas in an array configuration, loading a reflector layer, utilization of the shorting pins for optimizing the impedance matching of the planar antenna, the employment of high permittivity substrates, altering the basic shape of the antenna, as well as utilizing multiple substrates. On the other hand, it is expected that current methodologies, including the aforementioned ones, will be further enhanced by using modern approaches (e.g., artificial materials; MTMs), especially in terms of mitigating the drawbacks of the conventional methods such as the bulky structures, complex feed networks, and complex power distribution systems.
- Over the last decade, a great interest has been directed to enhancing antenna performance by exploiting the unique properties of MTMs. In this regard, the degrees

TABLE 3. Summary of gain improvement using MTM lens.

Ref.	Antenna type	Frequency (GHz)	Gain enhancement	Lensing property based on	No. of uint cells (No. of layers)	MTM structure
[115]	Antipodal exponential tapered slot antenna	7–12	9.5 dB	GRIN	32 × 32 (Six layer)	Rectangular rings
[116]	Antipodal tapered slot antenna	6–19	1.3–3.6 dB	$n_{MTM}>n_{air}$	36 (-)	Parallel lines shaped resonator
[117]	Bow-tie	5.1–8.3	1.5–3.5 dB	$n_{MTM}>n_{air}$	2 × 2 (-)	I-shape resonator (ISR) structure
[118]	Periodic end-fire antenna	3–11	2–3.5 dB	$n_{MTM}>n_{air}$	2 × 2 (-)	I-shape resonator (ISR) structure
[119]	Quasi-Yagi antenna	4.5–9.5	2 dBi	$n_{MTM}>n_{air}$	2 × 6 (-)	I-shaped resonator (ISR)
[121]	Planar log-periodic dipole array	26–40	4 dB	$n_{MTM}>n_{air}$	83 (-)	Metallic semi-ring structure
[122]	Dipole antenna	26–30	5dB	$n_{MTM}>n_{air}$	8 × 6 (-)	C- shaped resonator
[123]	Wideband End-fire antenna	5–11	2 dB	$n_{MTM}>n_{air}$	2 × 6 (-)	SRR
[136]	Tapered slot antenna	10	6 dB	GRIN	13 × 10 (7 layers)	Non-resonant parallel-line unit cell
[137]	Monopole antenna	3–8	10 dB	GRIN	32 × 32 (14 layers on each side)	Sierpinski fractal ring unit cell
[139]	Vivaldi antenna	10.5–12.5	4 dB (approx.)	GRIN	13 × 10 (One layer)	Complementary closed ring resonator (CCR)
[140]	Dielectric resonator antenna	3.1–4.1	6 dB	NRI	4 × 4 (One layer)	E-shaped resonator (ESR)
[141]	Dielectric resonator antenna	7.8	6.5 dBi	NRI	5 × 10 (One layer)	Infinity shaped resonator (ISR)
[142]	Vivaldi antenna	6.5–20	4 dB	NRI	3 × 4 (7 layers)	Negative index MTM structure
[143]	Patch antenna	28	5.35 dBi	NRI	3 × 4 (one layer)	VCSRM
[144]	Patch antenna	5.8	7.8 dBi	NRI	2 (one layer)	SRR and wire strips
[145]	Patch antenna	2.4	4 dB	NRI	1 × 7 (8 layers)	Modified square rectangular SRR
[146]	Patch antenna array	5.8	8 dBi	NRI	2 × 1 (one layer)	SRR
[147]	Microstrip antenna	902 MHz	4.07 dBi	NRI	2 × 4 (Two layers)	Jerusalem Cross unit cell
[148]	Cylindrical antenna	1.3–1.45	2–3.5 dB	NRI	7 × 7 (One layer)	Squared metal lattice
[149]	Patch antenna	3.6	4.1 dB	NRI	4 × 4 (4 layers)	Double negative MTM
[150]	Patch antenna array	5.68–6.05	1.68 dBi	NRI	2 × 4 (One layer)	Hexagonal nested loop
[151]	Patch antenna	11.4	2.9 dB	NRI	3 × 7 (One layer)	Minkowski Fractal shaped MTM
[152]	Microstrip antenna	2.5	3.69 dB	NRI	SRR unit cells (-)	Modified square SRR

of freedom available to the designer when using different properties of MTMs enable a broad range of enhancing scenarios.

- Many approaches to realization of gain improvement are based on the MTMs properties such as LIMs, ZIMs, MNZ, ENZ, low impedance MTMs, and MTM lenses ($n_{MTM} > n_{air}$, GRIN, and NRI). These characteristics of MTMs allow assembling radiated waves from the antenna and collimating them in the normal direction. This concept has already been validated in several designs at different frequency bands (microwave, millimetre-wave, and terahertz).

TABLE 4. Advantages and drawbacks of the antenna gain enhancement methods based on MTM characteristics.

Ref. No.	Gain enhancement approach	Advantages	drawbacks
[53], [73]– [88]	ZIMs, LIMs, or NZIMs	• High gain enhancement up to 8.57 dB with only one MTM layer. [73] • Gain enhancement mechanism is based on the principle of the Snell's law.	• The multi-layer of MTMs increases the size and complexity antenna system. [78],[79],[84] • Most of the presented reports used this approach to enhance only one feature of the antenna, which is the gain.
[66],[67], [106]– [110]	ENZ or MNZ	• Easy mechanism by using the principle of the Snell's law. • Freedom on optimizing either ε and μ with near-zero property.	• All presented reports used ENZ or MNZ to enhance the antenna performance in terms of gain improvement only. • These materials are not able to match the impedance of the air, which yields a significant reduction in the antenna efficiency.
[54],[68], [69],[112], [113]	Low impedance MTMs	• High gain enhancement up to 8.3 dB. [68] • Reduction of the overall size of the antenna system by minimizing the air-gap between the antenna and the MTM layer.	• The structure needs to be optimized to obtain both VLE and MNZ and thus low impedance property. • This approach is not as popular as others; only few reports were published in the literature thus far.
[115]–[119], [121]–[154]	MTM lens	• Freedom in designing MTM lens based on the three properties (HRI, GRIN, and NRI). • GRIN lens provides the highest gain enhancement up to 10 dB in comparison to other approaches. [137] • Different MTM lens characteristics help to improve the antenna performance in terms of gain, efficiency, and bandwidth, and reduce the overall size. • The MTM lens, GRIN, offers non-resonant, wide bandwidth, and low-loss behaviour compared to traditional lenses.	• The design process of the GRIN lenses is time-consuming, and, in most cases, the lenses are highly polarization-sensitive, • Using a large number of layers up to 14 increases the overall size and complexity of the GRIN lens. [137],[145]

- Miniaturization of antenna systems is instrumental in obtaining light-weight and portable devices. Compactness of the design along with improved performance can be achieved by the incorporation of MTMs. The low impedance MTM approach certainly has a great potential to provide significant gain improvement while reducing the overall size and complexity of the antenna system. In particular, the air gap between the antenna and the MTMs can be reduced to small values to yield a compact and high-performance system. This approach would require more investigation using the integration of different MTM shapes with various antennas.
- Gain enhancement based on MTMs depends on many factors like the number of unit cells, the air gap between the antenna and MTMs, and the printed unit cells on one or both sides of the substrate. In the broadside direction, MTMs, namely superstrate, are included at the front/above the radiating part of the antenna. In such a scenario, the number of layers and the distance between the radiating element and the MTM layer are essential to determine the enhanced gain. With the end-fire direction, MTMs are normally etched on the antenna substrate. The gain enhancement here is contingent upon the number of unit cells, and whether the unit cells are printed on one or both sides of the substrate.

The advantages and drawbacks of the gain enhancement approaches based on MTMs in the presented literature are tabulated in Table 4.

IV. CONCLUSION

This review provided an introduction to the MTMs and discussed their practical applications in the light of the available literature. Further, their classifications were presented as well. In more depth, the review highlighted the capability of MTMs to enhance the antenna's performance, in which various MTM properties such as ZIM, ENZ, and MNZ are used to improve the gain performance. These properties can improve the gain of a wide variety of planar antennas, where the principle of operation is based on the Snell's law of refraction. Moreover, the MTM with low impedance property was loaded to planar antennas for gain enhancement. Such property can be realized by a structure with VLE or MNZ, which simultaneously enhances the gain and reduces the overall antenna size. The lensing property of MTMs is another gain enhancement approach where it helps to focus the radiated beam from the antenna into the emission direction. A number of degrees of freedom are available to the designer when using this approach, where MTMs lens can be achieved by three different characteristics: HRI, GRIN, and NRI. The efficiency of antenna gain improvement based on MTMs would

depend on the number of layers, and the distance between the radiating element and the MTM layer when the MTMs are included in the front/above the radiating part of the antenna (broadside direction). In the case of etching the MTMs on the substrate, the gain enhancement relies on the number of unit cells and whether the unit cells print on one or both sides of the substrate (end-fire direction).

APPENDIX

NOMENCLATURE

MTMs	Metamaterials.
ZIM	Zero-index material.
ENZ	Epsilon-near-zero.
MNZ	Mu near-zero.
SRR	Split-ring resonator.
5G	Fifth-generation.
4G	Fourth-generation.
MIMO	Multiple-input-multiple-output.
FSS	Frequency Selective Surface.
EBG	Electromagnetic Band-Gap.
AMC	Artificial Magnetic Conductor.
SAR	Synthetic aperture radar.
LIM	Low-index material.
GRIN	Gradient refractive index.
DPS	Double-positive material.
ENG	Epsilon negative material.
MNG	Mu-negative material.
DNG	Double negative material.
LHMs	Left-handed materials.
VLE	Very large epsilon.
HRI	High refractive index.
GRIN	Gradient index.
NRI	Negative refractive index.
NZIM	Near zero-index material.
ELC	Electric-field-coupled.
AZIM	Anisotropic zero-index material.
ATSA	Antipodal tapered-slot antenna.
ELDR	Periodic end-loaded dipole resonator.
SIW	Substrate integrated waveguide.
DGRs	G-shaped resonators.
CVA	Conventional vivaldi antenna.
SR	Square-ring.
RSA	Ring slot antenna.
CCLR	Cross circular loop resonator.
SIW-SA	Substrate integrated waveguide fed-slot antenna.
CP	Circularly polarized.
HPBW	Half-power beamwidth.
ATSA	Antipodal tapered slot antenna.
ISR	I-shape resonator.
HSR	H-shaped resonator.
TSPM	Two-sided planar metamaterial.
TSA	Tapered slot antenna.
CCR	Complementary non-resonant closed ring.
DRA	Dielectric resonator antenna.
ESR	E-shaped resonator.
ISR	Infinity shape resonator.
MPA	Microstrip patch antenna.
VCSRM	Vertically coupled split ring metaplate.

REFERENCES

[1] S. Zhang, W. Fan, N. C. Panoiu, K. J. Malloy, R. M. Osgood, and S. R. J. Brueck, "Experimental demonstration of near-infrared negative-index metamaterials," *Phys. Rev. Lett.*, vol. 95, no. 13, Sep. 2005, Art. no. 137404.

[2] M. S. Islam, M. Samsuzzaman, G. K. Beng, N. Misran, N. Amin, and M. T. Islam, "A gap coupled hexagonal split ring resonator based metamaterial for S-band and X-band microwave applications," *IEEE Access*, vol. 8, pp. 68239–68253, 2020.

[3] V. G. Veselago, "The electrodynamics of substances with simultaneous negative values of ε and μ," *Sov. Phys. Uspekhi*, vol. 10, no. 4, pp. 509–514, 1968.

[4] J. B. Pendry, A. J. Holden, W. J. Stewart, and I. Youngs, "Extremely low frequency plasmons in metallic mesostructures," *Phys. Rev. Lett.*, vol. 76, no. 25, pp. 4773–4776, Jun. 1996.

[5] J. B. Pendry, A. J. Holden, D. J. Robbins, and W. J. Stewart, "Magnetism from conductors and enhanced nonlinear phenomena," *IEEE Trans. Microw. Theory Techn.*, vol. 47, no. 11, pp. 2075–2084, Nov. 1999.

[6] D. R. Smith, W. J. Padilla, D. C. Vier, S. C. Nemat-Nasser, and S. Schultz, "Composite medium with simultaneously negative permeability and permittivity," *Phys. Rev. Lett.*, vol. 84, no. 18, pp. 4184–4187, May 2000.

[7] S. Haxha, F. AbdelMalek, F. Ouerghi, M. D. B. Charlton, A. Aggoun, and X. Fang, "Metamaterial superlenses operating at visible wavelength for imaging applications," *Sci. Rep.*, vol. 8, no. 1, pp. 1–15, Dec. 2018.

[8] M. Chen, H. Jiang, H. Zhang, D. Li, and Y. Wang, "Design of an acoustic superlens using single-phase metamaterials with a star-shaped lattice structure," *Sci. Rep.*, vol. 8, no. 1, pp. 1–8, Dec. 2018.

[9] S. Khosravi, A. Rostami, M. Dolatyari, and G. Rostami, "Broadband carpet cloak designed using nanocomposite metamaterials for 3–5-μm wavelength range," *IEEE Trans. Nanotechnol.*, vol. 16, no. 1, pp. 44–48, Jan. 2017.

[10] H. K. Zhang, Y. Chen, X. N. Liu, and G. K. Hu, "An asymmetric elastic metamaterial model for elastic wave cloaking," *J. Mech. Phys. Solids*, vol. 135, pp. 1–12, Feb. 2020.

[11] C. Qian and H. Chen, "A perspective on the next generation of invisibility cloaks—Intelligent cloaks," *Appl. Phys. Lett.*, vol. 118, no. 18, pp. 1–8, 2021.

[12] K. Aydin, I. Bulu, and E. Ozbay, "Subwavelength resolution with a negative-index metamaterial superlens," *Appl. Phys. Lett.*, vol. 90, no. 25, pp. 1–3, 2007.

[13] S. H. Sedighy, C. Guclu, S. Campione, M. K. Amirhosseini, and F. Capolino, "Wideband planar transmission line hyperbolic metamaterial for subwavelength focusing and resolution," *IEEE Trans. Microw. Theory Techn.*, vol. 61, no. 12, pp. 4110–4117, Dec. 2013.

[14] E. Ahamed, M. R. I. Faruque, M. J. Alam, M. F. B. Mansor, and M. T. Islam, "Digital metamaterial filter for encoding information," *Sci. Rep.*, vol. 10, no. 1, pp. 1–9, Dec. 2020.

[15] Y. Meng, J. Wang, H. Chen, L. Zheng, H. Ma, and S. Qu, "Countering single-polarization radar based on polarization conversion metamaterial," *IEEE Access*, vol. 8, pp. 206783–206789, 2020.

[16] L. Yan, Z. He, W. Jiang, and X. Zheng, "Design of the broadband metamaterial absorber based on dispersed carbon fibers in oblique incidence," *IEEE Access*, vol. 8, pp. 214775–214780, 2020.

[17] B. A. Esmail, H. B. Majid, Z. B. Z. Abidin, S. H. B. Dahlan, M. Himdi, M. R. Kamarudin, and M. K. Rahim, "Dual mode modified double square ring resonator structure at 76 GHz," *Microw. Opt. Technol. Lett.*, vol. 61, no. 7, pp. 1678–1682, Jul. 2019.

[18] B. A. F. Esmail, H. A. Majid, F. A. Saparudin, M. Jusoh, A. Y. Ashyap, N. Al-Fadhali, and M. K. A. Rahim, "Negative refraction metamaterial with low loss property at millimeter wave spectrum," *Bull. Electr. Eng. Informat.*, vol. 9, no. 3, pp. 1038–1045, Jun. 2020.

[19] Z. He, J. Jin, Y. Zhang, and Y. Duan, "Design of a two-dimensional 'T' shaped metamaterial with wideband, low loss," *IEEE Trans. Appl. Supercond.*, vol. 29, no. 2, pp. 1–4, Mar. 2019.

[20] H. Liu, S. Lei, X. Shi, and L. Li, "Study of antenna superstrates using metamaterials for directivity enhancement based on Fabry–Pérot resonant cavity," *Int. J. Antennas Propag.*, vol. 2013, pp. 1–10, Feb. 2013.

[21] B. Ma, X.-M. Yang, T.-Q. Li, X.-F. Du, M.-Y. Yong, H.-Y. Chen, H. He, Y.-W. Chen, A. Lin, J. Chen, and L. Zhou, "Gain enhancement of transmitting antenna incorporated with double-cross-shaped electromagnetic metamaterial for wireless power transmission," *Optik*, vol. 127, no. 16, pp. 6754–6762, Aug. 2016.

[22] M. Alibakhshikenari, B. S. Virdee, P. Shukla, Y. Wang, L. Azpilicueta, M. Naser-Moghadasi, C. H. See, I. Elfergani, C. Zebiri, R. A. Abd-Alhameed, I. Huynen, J. Rodriguez, T. A. Denidni, F. Falcone, and E. Limiti, "Impedance bandwidth improvement of a planar antenna based on metamaterial-inspired T-matching network," *IEEE Access*, vol. 9, pp. 67916–67927, 2021.

[23] Y. Cho, J. J. Kim, D. H. Kim, S. Lee, H. Kim, C. Song, S. Kong, H. Kim, C. Seo, S. Ahn, and J. Kim, "Thin PCB-type metamaterials for improved efficiency and reduced EMF leakage in wireless power transfer systems," *IEEE Trans. Microw. Theory Techn.*, vol. 64, no. 2, pp. 353–364, Feb. 2016.

[24] T. Cai, G.-M. Wang, X.-F. Zhang, Y.-W. Wang, B.-F. Zong, and H.-X. Xu, "Compact microstrip antenna with enhanced bandwidth by loading magneto-electro-dielectric planar waveguided metamaterials," *IEEE Trans. Antennas Propag.*, vol. 63, no. 5, pp. 2306–2311, May 2015.

[25] B. A. F. Esmail, H. B. Majid, S. H. Dahlan, Z. Z. Abidin, M. K. A. Rahim, and M. Jusoh, "Planar antenna beam deflection using low-loss metamaterial for future 5G applications," *Int. J. RF Microw. Comput.-Aided Eng.*, vol. 29, no. 10, pp. 1–11, Oct. 2019.

[26] B. A. F. Esmail, H. A. Majid, S. H. Dahlan, Z. Z. Abidin, M. Himdi, R. Dewan, M. K. A. Rahim, and A. Y. I. Ashyap, "Reconfigurable metamaterial structure for 5G beam tilting antenna applications," *Waves Random Complex Media*, vol. 31, no. 6, pp. 2089–2102, Nov. 2021.

[27] M. Alibakhshikenari, M. Khalily, B. S. Virdee, C. H. See, R. Abd-Alhameed, and E. Limiti, "Mutual coupling suppression between two closely placed microstrip patches using EM-bandgap metamaterial fractal loading," *IEEE Access*, vol. 7, pp. 23606–23614, 2019.

[28] M. Alibakhshikenari, B. S. Virdee, P. Shukla, N. O. Parchin, L. Azpilicueta, C. H. See, R. A. Abd-Alhameed, F. Falcone, I. Huynen, T. A. Denidni, and E. Limiti, "Metamaterial-inspired antenna array for application in microwave breast imaging systems for tumor detection," *IEEE Access*, vol. 8, pp. 174667–174678, 2020.

[29] B. A. F. Esmail, H. A. Majid, Z. Z. Abidin, S. H. Dahlan, M. Himdi, R. Dewan, M. K. Rahim, and N. Al-Fadhali, "Reconfigurable radiation pattern of planar antenna using metamaterial for 5G applications," *Materials*, vol. 13, no. 3, pp. 1–15, 2020.

[30] H. Jiang, L.-M. Si, W. Hu, and X. Lv, "A symmetrical dual-beam bowtie antenna with gain enhancement using metamaterial for 5G MIMO applications," *IEEE Photon. J.*, vol. 11, no. 1, pp. 1–9, Feb. 2019.

[31] B. A. F. Esmail, H. A. Majid, S. H. Dahlan, Z. Z. Abidin, M. K. A. Rahim, M. A. Abdullah, and M. Jusoh, "Antenna beam tilting and gain enhancement using novel metamaterial structure at 28 GHz," in *Proc. IEEE Int. RF Microw. Conf. (RFM)*, Penang, Malaysia, Dec. 2018, pp. 53–56.

[32] H. Guo and W. Geyi, "Design of bidirectional antenna array with adjustable endfire gains," *IEEE Antennas Wireless Propag. Lett.*, vol. 18, no. 8, pp. 1656–1660, Aug. 2019.

[33] H.-J. Dong, Y.-B. Kim, J. Joung, and H. L. Lee, "High gain and low-profile stacked magneto-electric dipole antenna for phased array beamforming," *IEEE Access*, vol. 8, pp. 180295–180304, 2020.

[34] L. Ge and K.-M. Luk, "A low-profile magneto-electric dipole antenna," *IEEE Trans. Antennas Propag.*, vol. 60, no. 4, pp. 1684–1689, Apr. 2012.

[35] A. S. Mekki, M. N. Hamidon, A. Ismail, and A. R. H. Alhawari, "Gain enhancement of a microstrip patch antenna using a reflecting layer," *Int. J. Antennas Propag.*, vol. 2015, pp. 1–7, Oct. 2015.

[36] X. Zhang and L. Zhu, "Gain-enhanced patch antenna without enlarged size via loading of slot and shorting pins," *IEEE Trans. Antennas Propag.*, vol. 65, no. 11, pp. 5702–5709, Nov. 2017.

[37] X. Zhang and L. Zhu, "Gain-enhanced patch antennas with loading of shorting pins," *IEEE Trans. Antennas Propag.*, vol. 64, no. 8, pp. 3310–3318, Aug. 2016.

[38] S. Aditya, C. K. Sim, D. Wu, W. T. Chua, Z. X. Shen, and C. L. Law, "High-gain 24-GHz CPW-fed microstrip patch antennas on high-permittivity substrates," *IEEE Antennas Wireless Propag. Lett.*, vol. 3, pp. 30–33, 2004.

[39] A. Abdel-Rahman, A. K. Verma, and A. S. Omar, "High gain microstrip antenna element and array on low and high permittivity substrate," in *Proc. Eur. Microw. Conf.*, Paris, France, Oct. 2005, pp. 487–489.

[40] K. Sharma, D. K. Upadhyay, and H. Parthasarathy, "Modified circular-shaped microstrip patch antenna," in *Proc. IEEE Int. Conf. Comput. Intell. Commun. Technol.*, Ghaziabad, India, Feb. 2015, pp. 397–399.

[41] M. M. Honari, A. Abdipour, and G. Moradi, "Bandwidth and gain enhancement of an aperture antenna with modified ring patch," *IEEE Antennas Wireless Propag. Lett.*, vol. 10, pp. 1413–1416, 2011.

[42] G. Montisci, Z. Jin, M. Li, H. Yang, G. A. Casula, G. Mazzarella, and A. Fanti, "Design of multilayer dielectric cover to enhance gain and efficiency of slot arrays," *Int. J. Antennas Propag.*, vol. 2013, pp. 1–6, Jan. 2013.

[43] D. C. Lugo, R. A. Ramirez, J. Wang, and T. M. Weller, "Multilayer dielectric end-fire antenna with enhanced gain," *IEEE Antennas Wireless Propag. Lett.*, vol. 17, no. 12, pp. 2213–2217, Dec. 2018.

[44] M. Asaadi, I. Afifi, and A.-R. Sebak, "High gain and wideband high dense dielectric patch antenna using FSS superstrate for millimeter-wave applications," *IEEE Access*, vol. 6, pp. 38243–38250, 2018.

[45] J. Li, Q. Zeng, R. Liu, and T. A. Denidni, "A gain enhancement and flexible control of beam numbers antenna based on frequency selective surfaces," *IEEE Access*, vol. 6, pp. 6082–6091, 2018.

[46] Y. Yuan, X. Xi, and Y. Zhao, "Compact UWB FSS reflector for antenna gain enhancement," *IET Microw., Antennas Propag.*, vol. 13, no. 10, pp. 1749–1755, Aug. 2019.

[47] M. S. Khan, F. A. Tahir, A. Meredov, A. Shamim, and H. M. Cheema, "A W-band EBG-backed double-rhomboid bowtie-slot on-chip antenna," *IEEE Antennas Wireless Propag. Lett.*, vol. 18, no. 5, pp. 1046–1050, May 2019.

[48] D. Chen, W. Yang, and W. Che, "High-gain patch antenna based on cylindrically projected EBG planes," *IEEE Antennas Wireless Propag. Lett.*, vol. 17, no. 12, pp. 2374–2378, Dec. 2018.

[49] T. Wu, J. Chen, and M.-J. Wang, "Multi-state circularly polarized antenna based on the polarization conversion metasurface with gain enhancement," *IEEE Access*, vol. 8, pp. 84660–84666, 2020.

[50] K. Li, Y. Liu, Y. Jia, and Y. J. Guo, "A circularly polarized high-gain antenna with low RCS over a wideband using chessboard polarization conversion metasurfaces," *IEEE Trans. Antennas Propag.*, vol. 65, no. 8, pp. 4288–4292, Aug. 2017.

[51] Y. Gong, S. Yang, B. Li, Y. Chen, F. Tong, and C. Yu, "Multi-band and high gain antenna using AMC ground characterized with four zero-phases of reflection coefficient," *IEEE Access*, vol. 8, pp. 171457–171468, 2020.

[52] S. Yang, Y. Chen, C. Yu, Y. Gong, and F. Tong, "Design of a low-profile, frequency- reconfigurable, and high gain antenna using a varactor-loaded AMC ground," *IEEE Access*, vol. 8, pp. 158635–158646, 2020.

[53] H. Zhou, Z. Pei, S. Qu, S. Zhang, J. Wang, Z. Duan, H. Ma, and Z. Xu, "A novel high-directivity microstrip patch antenna based on zero-index metamaterial," *IEEE Antennas Wireless Propag. Lett.*, vol. 8, pp. 538–541, 2009.

[54] M. Zada, I. A. Shah, and H. Yoo, "Metamaterial-loaded compact high-gain dual-band circularly polarized implantable antenna system for multiple biomedical applications," *IEEE Trans. Antennas Propag.*, vol. 68, no. 2, pp. 1140–1144, Feb. 2020.

[55] M. Alibakhshikenari, B. S. Virdee, L. Azpilicueta, M. Naser-Moghadasi, M. O. Akinsolu, C. H. See, B. Liu, R. A. Abd-Alhameed, F. Falcone, I. Huynen, and T. A. Denidni, "A comprehensive survey of 'metamaterial transmission-line based antennas: Design, challenges, and applications,'" *IEEE Access*, vol. 8, pp. 144778–144808, 2020.

[56] M. Alibakhshikenari, F. Babaeian, B. S. Virdee, S. Aïssa, L. Azpilicueta, C. H. See, A. A. Althuwayb, I. Huynen, R. A. Abd-Alhameed, F. Falcone, and E. Limiti, "A comprehensive survey on 'various decoupling mechanisms with focus on metamaterial and metasurface principles applicable to SAR and MIMO antenna systems,'" *IEEE Access*, vol. 8, pp. 192965–193004, 2020.

[57] Y. Liu and X. Zhang, "Metamaterials: A new frontier of science and technology," *Chem. Soc. Rev.*, vol. 40, no. 5, pp. 2494–2507, Dec. 2011.

[58] Y. T. Aladadi and M. A. S. Alkanhal, "Extraction of metamaterial constitutive parameters based on data-driven discontinuity detection," *Opt. Mater. Exp.*, vol. 9, no. 9, pp. 3765–3780, 2019.

[59] T. M. Grzegorczyk, C. D. Moss, J. Lu, X. Chen, J. Pacheco, and J. A. Kong, "Properties of left-handed metamaterials: Transmission, backward phase, negative refraction, and focusing," *IEEE Trans. Microw. Theory Techn.*, vol. 53, no. 9, pp. 2956–2967, Sep. 2005.

[60] S. H. Lee, C. M. Park, Y. M. Seo, and C. K. Kim, "Reversed Doppler effect in double negative metamaterials," *Phys. Rev. B, Condens. Matter*, vol. 81, no. 24, pp. 1–4, Jun. 2010.

[61] S. Xi, H. Chen, T. Jiang, L. Ran, J. Huangfu, B.-I. Wu, J. A. Kong, and M. Chen, "Experimental verification of reversed Cherenkov radiation in left-handed metamaterial," *Phys. Rev. Lett.*, vol. 103, no. 19, pp. 1–4, Nov. 2009.

[62] J. B. Pendry, A. J. Holden, D. J. Robbins, and W. J. Stewart, "Low frequency plasmons in thin-wire structures," *J. Phys. Condens. Matter*, vol. 10, no. 22, pp. 4785–4809, Jun. 1998.

[63] J. D. Jackson, *Classical Electromagnetics*, 3rd ed. New York, NY, USA: Wiley, 1999.

[64] S. Islam, M. Faruque, and M. Islam, "A near zero refractive index metamaterial for electromagnetic invisibility cloaking operation," *Materials*, vol. 8, no. 8, pp. 4790–4804, Jul. 2015.

[65] H. F. Ma, J. H. Shi, W. X. Jiang, and T. J. Cui, "Experimental realization of bending waveguide using anisotropic zero-index materials," *Appl. Phys. Lett.*, vol. 101, no. 25, pp. 1–4, 2012.

[66] C. Cheng, Y. Lu, D. Zhang, F. Ruan, and G. Li, "Gain enhancement of terahertz patch antennas by coating epsilon-near-zero metamaterials," *Superlattices Microstruct.*, vol. 139, pp. 1–8, Mar. 2020.

[67] D. Gangwar, S. Das, and R. L. Yadava, "Gain enhancement of microstrip patch antenna loaded with split ring resonator based relative permeability near zero as superstrate," *Wireless Pers. Commun.*, vol. 96, no. 2, pp. 2389–2399, Sep. 2017.

[68] S. Pandit, A. Mohan, and P. Ray, "Square-ring metamaterial for radiation characteristics enhancement of an SIW cavity-backed slot antenna," *Int. J. RF Microw. Comput.-Aided Eng.*, vol. 30, no. 2, pp. 1–8, Feb. 2020.

[69] D. Mitra, B. Ghosh, A. Sarkhel, and S. R. B. Chaudhuri, "A miniaturized ring slot antenna design with enhanced radiation characteristics," *IEEE Trans. Antennas Propag.*, vol. 64, no. 1, pp. 300–305, Jan. 2016.

[70] F. Khajeh-Khalili, M. A. Honarvar, and A. Dadgarpour, "High-gain bow-tie antenna using array of two-sided planar metamaterial loading for *H*-band applications," *Int. J. RF Microw. Comput.-Aided Eng.*, vol. 28, no. 7, pp. 1–7, 2018.

[71] X. Niu, X. Hu, S. Chu, and Q. Gong, "Epsilon-near-zero photonics: A new platform for integrated devices," *Adv. Opt. Mater.*, vol. 6, no. 10, pp. 1–36, 2018.

[72] I. Liberal and N. Engheta, "Near-zero refractive index photonics," *Nature Photon.*, vol. 11, no. 3, pp. 149–158, Mar. 2017.

[73] A. Bakhtiari, "Investigation of enhanced gain miniaturized patch antenna using near zero index metamaterial structure characteristics," *IETE J. Res.*, pp. 1–8, 2019, doi: 10.1080/03772063.2019.1644973.

[74] M. Bayat and J. Khalilpour, "A high gain miniaturised patch antenna with an epsilon near zero superstrate," *Mater. Res. Exp.*, vol. 6, no. 4, pp. 1–9, 2020.

[75] J. Ju, D. Kim, W. J. Lee, and J. I. Choi, "Wideband high-gain antenna using metamaterial superstrate with the zero refractive index," *Microw. Opt. Technol. Lett.*, vol. 51, no. 8, pp. 1973–1976, Aug. 2009.

[76] D. Li, Z. Szabo, X. Qing, E.-P. Li, and Z. N. Chen, "A high gain antenna with an optimized metamaterial inspired superstrate," *IEEE Trans. Antennas Propag.*, vol. 60, no. 12, pp. 6018–6023, Dec. 2012.

[77] M. Bouzouad, S. M. Chaker, D. Bensafielddine, and E. M. Laamari, "Gain enhancement with near-zero-index metamaterial superstrate," *Appl. Phys. A, Solids Surf.*, vol. 121, no. 3, pp. 1075–1080, Nov. 2015.

[78] B. Zhou and T. J. Cui, "Directivity enhancement to Vivaldi antennas using compactly anisotropic zero-index metamaterials," *IEEE Antennas Wireless Propag. Lett.*, vol. 10, pp. 326–329, 2011.

[79] B. Zhou, H. Li, X. Y. Zou, and T.-J. Cui, "Broadband and high-gain planar Vivaldi antennas based on inhomogeneous anisotropic zero-index metamaterials," *Prog. Electromagn. Res.*, vol. 120, pp. 235–247, 2011.

[80] M. Bhaskar, E. Johari, Z. Akhter, and M. J. Akhtar, "Gain enhancement of the Vivaldi antenna with band notch characteristics using zero-index metamaterial," *Microw. Opt. Technol. Lett.*, vol. 58, no. 1, pp. 233–238, Jan. 2016.

[81] R.-C. Deng, X.-M. Yang, B. Ma, T.-Q. Li, H.-Y. Chen, Y. Yang, H. He, Y.-W. Chen, and Z. Tang, "Performance enhancement of novel antipodal Vivaldi antenna with irregular spacing distance slots and modified-w-shaped metamaterial loading," *Appl. Phys. A, Solids Surf.*, vol. 125, no. 1, pp. 1–11, Jan. 2019.

[82] M. Sun, Z. N. Chen, and X. Qing, "Gain enhancement of 60-GHz antipodal tapered slot antenna using zero-index metamaterial," *IEEE Trans. Antennas Propag.*, vol. 61, no. 4, pp. 1741–1746, Apr. 2013.

[83] M. Sun, Z. N. Chen, and X. Qing, "Gain enhancement of antipodal tapered slot antenna using zero-index metamaterial," in *Proc. IEEE Asia–Pacific Conf. Antennas Propag.*, Singapore, Aug. 2012, pp. 70–71.

[84] Z. H. Jiang, Q. Wu, D. E. Brocker, P. E. Sieber, and D. H. Werner, "A low-profile high-gain substrate-integrated waveguide slot antenna enabled by an ultrathin anisotropic zero-index metamaterial coating," *IEEE Trans. Antennas Propag.*, vol. 62, no. 3, pp. 1173–1184, Mar. 2014.

[85] T. Shaw, D. Bhattacharjee, and D. Mitra, "Gain enhancement of slot antenna using zero-index metamaterial superstrate," *Int. J. RF Microw. Comput.-Aided Eng.*, vol. 27, no. 4, pp. 1–10, 2017.

[86] A. Dadgarpour, B. Zarghooni, B. S. Virdee, and T. A. Denidni, "Millimeter-wave high-gain SIW end-fire bow-tie antenna," *IEEE Trans. Antennas Propag.*, vol. 63, no. 5, pp. 2337–2342, May 2015.

[87] M. Aeini, S. Jarchi, and R. Faraji-Dana, "Compact, wideband-printed quasi-Yagi antenna using spiral metamaterial resonators," *Electron. Lett.*, vol. 53, no. 21, pp. 1393–1394, Oct. 2017.

[88] F.-Y. Meng, Y.-L. Li, K. Zhang, Q. Wu, and J. L.-W. Li, "A detached zero index metamaterial lens for antenna gain enhancement," *Prog. Electromagn. Res.*, vol. 132, pp. 463–478, 2012.

[89] H. Suthar, D. Sarkar, K. Saurav, and K. V. Srivastava, "Gain enhancement of microstrip patch antenna using near-zero index metamaterial (NZIM) lens," in *Proc. 20st Nat. Conf. Commun. (NCC)*, Mumbai, India, Feb. 2015, pp. 1–6.

[90] A. Al-Saman, M. Cheffena, O. Elijah, Y. A. Al-Gumaei, S. K. A. Rahim, and T. Al-Hadhrami, "Survey of millimeter-wave propagation measurements and models in indoor environments," *Electronics*, vol. 10, no. 14, pp. 1–28, 2021.

[91] A. Palomares-Caballero, A. Alex-Amor, J. Valenzuela-Valdes, and P. Padilla, "Millimeter-wave 3-D-printed antenna array based on gap-waveguide technology and split E-plane waveguide," *IEEE Trans. Antennas Propag.*, vol. 69, no. 1, pp. 164–172, Jan. 2021.

[92] *Studies on Frequency-Related Matters for International Mobile Telecommunications Identification Including Possible Additional Allocations to the Mobile Services on a Primary Basis in Portion(s) of the Frequency Range Between 24.25 and 86 GHz for the Future Development of International Mobile Telecommunications for 2020 and Beyond*, World Radiocommun. Conf. Geneva, Switzerland, document RESOLUTION 238 (WRC-15), 2015, pp. 424–426.

[93] Q. L. Zhang, B. J. Chen, K. F. Chan, and C. H. Chan, "High-gain millimeter-wave antennas based on spoof surface plasmon polaritons," *IEEE Trans. Antennas Propag.*, vol. 68, no. 6, pp. 4320–4331, Jun. 2020.

[94] A. M. Al-samman, T. A. Rahman, and M. H. Azmi, "Indoor corridor wideband radio propagation measurements and channel models for 5G millimeter wave wireless communications at 19 GHz, 28 GHz, and 38 GHz bands," *Wireless Commun. Mobile Comput.*, vol. 2018, pp. 1–12, Mar. 2018.

[95] D. Chizhik, J. Du, R. Feick, M. Rodriguez, G. Castro, and R. A. Valenzuela, "Path loss and directional gain measurements at 28 GHz for non-line-of-sight coverage of indoors with corridors," *IEEE Trans. Antennas Propag.*, vol. 68, no. 6, pp. 4820–4830, Jun. 2020.

[96] Z. Tao, D. Bao, H. X. Xu, H. F. Ma, W. X. Jiang, and T. J. Cui, "A millimeter-wave system of antenna array and metamaterial lens," *IEEE Antennas Wireless Propag. Lett.*, vol. 15, pp. 370–373, 2016.

[97] S. S. Al-Bawri, M. T. Islam, T. Shabbir, G. Muhammad, M. S. Islam, and H. Y. Wong, "Hexagonal shaped near zero index (NZI) metamaterial based MIMO antenna for millimeter-wave application," *IEEE Access*, vol. 8, pp. 181003–181013, 2020.

[98] M. Farahani, J. Pourahmadazar, M. Akbari, M. Nedil, A. R. Sebak, and T. A. Denidni, "Mutual coupling reduction in millimeter-wave MIMO antenna array using a metamaterial polarization-rotator wall," *IEEE Antennas Wireless Propag. Lett.*, vol. 16, pp. 2324–2327, 2017.

[99] F. Khajeh-Khalili, M. A. Honarvar, M. Naser-Moghadasi, and M. Dolatshahi, "A simple method to enhance gain and isolation of MIMO antennas simultaneously based on metamaterial structures for millimeter-wave applications," *J. Infr., Millim., THz Waves*, vol. 42, pp. 1078–1093, Dec. 2021.

[100] A. Dadgarpour, B. Zarghooni, B. S. Virdee, and T. A. Denidni, "Improvement of gain and elevation tilt angle using metamaterial loading for millimeter-wave applications," *IEEE Antennas Wireless Propag. Lett.*, vol. 15, pp. 418–420, 2015.

[101] A. Dadgarpour, B. Zarghooni, B. S. Virdee, and T. A. Denidni, "One- and two-dimensional beam-switching antenna for millimeter-wave MIMO applications," *IEEE Trans. Antennas Propag.*, vol. 64, no. 2, pp. 564–573, Feb. 2016.

[102] S. El-Nady, R. R. Elsharkawy, A. I. Afifi, A. El-Hameed, and S. Anwer, "Performance improvement of substrate integrated cavity fed dipole array antenna using ENZ metamaterial for 5G applications," *Sensors*, vol. 22, no. 1, pp. 1–12, 2022.
[103] Y. G. Ma, P. Wang, X. Chen, and C. K. Ong, "Near-field plane-wave-like beam emitting antenna fabricated by anisotropic metamaterial," *Appl. Phys. Lett.*, vol. 94, no. 4, pp. 39–42, 2009, doi: 10.1063/1.3077128.
[104] Q. Cheng, W. X. Jiang, and T. J. Cui, "Radiation of planar electromagnetic waves by a line source in anisotropic metamaterials," *J. Phys. D, Appl. Phys.*, vol. 43, no. 33, Aug. 2010, Art. no. 335406.
[105] M. Alibakhshi-Kenari, M. Naser-Moghadasi, and R. A. Sadeghzadeh, "Bandwidth and radiation specifications enhancement of monopole antennas loaded with split ring resonators," *IET Microw., Antennas Propag.*, vol. 9, no. 14, pp. 1487–1496, Nov. 2015.
[106] A. H. Abdelgwad and T. M. Said, "High performance microstrip monopole antenna with loaded metamaterial wire medium superstrate," *Int. J. RF Microw. Comput.-Aided Eng.*, vol. 29, no. 5, pp. 1–9, 2019.
[107] N. N. Yoon, N. Ha-Van, and C. Seo, "High-gain and wideband aperture coupled feed patch antenna using four split ring resonators," *Microw. Opt. Technol. Lett.*, vol. 60, no. 8, pp. 1997–2001, Aug. 2018.
[108] S. El-Nady, H. M. Zamel, M. Hendy, A. H. A. Zekry, and A. M. Attiya, "Gain enhancement of a millimeter wave antipodal Vivaldi antenna by epsilon-near-zero metamaterial," *Prog. Electromagn. Res. C*, vol. 85, pp. 105–116, 2018.
[109] G. K. Pandey, H. S. Singh, and M. K. Meshram, "Meander-line-based inhomogeneous anisotropic artificial material for gain enhancement of UWB Vivaldi antenna," *Appl. Phys. A, Solids Surf.*, vol. 122, no. 2, pp. 1–9, Feb. 2016.
[110] A. Dadgarpour, A. A. Kishk, and T. A. Denidni, "Gain enhancement of planar antenna enabled by array of split-ring resonators," *IEEE Trans. Antennas Propag.*, vol. 64, no. 8, pp. 3682–3687, Aug. 2016.
[111] G. Lovat, P. Burghignoli, F. Capolino, and D. R. Jackson, "Combinations of low/high permittivity and/or permeability substrates for highly directive planar metamaterial antennas," *IET Microw., Antennas Propag.*, vol. 1, no. 1, pp. 177–183, 2007.
[112] S. Pandit, A. Mohan, and P. Ray, "Metamaterial-inspired low-profile high-gain slot antenna," *Microw. Opt. Technol. Lett.*, vol. 61, no. 9, pp. 2068–2073, Sep. 2019.
[113] S. Pandit, A. Mohan, and P. Ray, "A low-profile high-gain substrate-integrated waveguide-slot antenna with suppressed cross polarization using metamaterial," *IEEE Antennas Wireless Propag. Lett.*, vol. 16, pp. 1614–1617, 2017.
[114] T. A. Rhys, "The design of radially symmetric lenses," *IEEE Trans. Antennas Propag.*, vol. AP-18, no. 4, pp. 497–506, Jul. 1970.
[115] E. Erfani, M. Niroo-Jazi, and S. Tatu, "A high-gain broadband gradient refractive index metasurface lens antenna," *IEEE Trans. Antennas. Propag.*, vol. 64, no. 5, pp. 1968–1973, May 2016.
[116] L. Chen, Z. Lei, R. Yang, J. Fan, and X. Shi, "A broadband artificial material for gain enhancement of antipodal tapered slot antenna," *IEEE Trans. Antennas Propag.*, vol. 63, no. 1, pp. 395–400, Jan. 2015.
[117] W. Cao, B. Zhang, A. Liu, T. Yu, D. Guo, and Y. Wei, "Broadband high-gain periodic endfire antenna by using I-shaped resonator (ISR) structures," *IEEE Antennas Wireless Propag. Lett.*, vol. 11, pp. 1470–1473, 2012.
[118] Y. Sun, Z. Du, J. Du, Y. Liu, and M. A. Basit, "Enhanced gain and broadband of endfire antenna by using I-shaped resonator structures," *Int. J. RF Microw. Comput.-Aided Eng.*, vol. 28, no. 7, pp. 1–6, 2018.
[119] Y. H. Sun, G. J. Wen, H. Y. Jin, P. Wang, and Y. J. Huang, "Gain enhancement for wide bandwidth endfire antenna with I-shaped resonator (ISR) structures," *Electron. Lett.*, vol. 49, no. 12, pp. 736–737, Jun. 2013.
[120] H. Wang, S.-F. Liu, L. Chen, W.-T. Li, and X.-W. Shi, "Gain enhancement for broadband vertical planar printed antenna with H-shaped resonator structures," *IEEE Trans. Antennas Propag.*, vol. 62, no. 8, pp. 4411–4415, Aug. 2014.
[121] G. Zhai, X. Wang, R. Xie, J. Shi, J. Gao, B. Shi, and J. Ding, "Gain-enhanced planar log-periodic dipole array antenna using nonresonant metamaterial," *IEEE Trans. Antennas Propag.*, vol. 67, no. 9, pp. 6193–6198, Sep. 2019.
[122] Z. Wani, M. P. Abegaonkar, and S. K. Koul, "Gain enhancement of millimeter wave antenna with metamaterial loading," in *Proc. Int. Symp. Antennas Propag. (ISAP)*, Phuket, Thailand, Oct. 2017, pp. 1–2.
[123] M. Wei, Y. Sun, X. Wu, and W. Wen, "Gain enhancement for wideband end-fire antenna design with artificial material," *SpringerPlus*, vol. 5, no. 1, pp. 1–9, Dec. 2016.
[124] X.-Y. He, Q. Chen, L.-C. Li, C. Yang, B. Li, B.-H. Zhou, and C.-X. Tang, "Nonresonant metamaterials with an ultra-high permittivity," *Chin. Phys. Lett.*, vol. 28, no. 5, pp. 9–12, 2011.
[125] H. F. Ma, B. G. Cai, T. X. Zhang, Y. Yang, W. X. Jiang, and T. J. Cui, "Three-dimensional gradient-index materials and their applications in microwave lens antennas," *IEEE Trans. Antennas Propag.*, vol. 61, no. 5, pp. 2561–2569, May 2013.
[126] C. Milias, R. B. Andersen, P. I. Lazaridis, Z. D. Zaharis, B. Muhammad, J. T. B. Kristensen, A. Mihovska, and D. D. S. Hermansen, "Metamaterial-inspired antennas: A review of the state of the art and future design challenges," *IEEE Access*, vol. 9, pp. 89846–89865, 2021.
[127] S. Zhang, R. K. Arya, W. G. Whittow, D. Cadman, R. Mittra, and J. C. Vardaxoglou, "Ultra-wideband flat metamaterial GRIN lenses assisted with additive manufacturing technique," *IEEE Trans. Antennas Propag.*, vol. 69, no. 7, pp. 3788–3799, Jul. 2021.
[128] Z. Tao, W. X. Jiang, H. F. Ma, and T. J. Cui, "High-gain and high-efficiency GRIN metamaterial lens antenna with uniform amplitude and phase distributions on aperture," *IEEE Trans. Antennas Propag.*, vol. 66, no. 1, pp. 16–22, Jan. 2018.
[129] A. Dadgarpour, B. Zarghooni, B. S. Virdee, and T. A. Denidni, "Beam-deflection using gradient refractive-index media for 60-GHz end-fire antenna," *IEEE Trans. Antennas Propag.*, vol. 63, no. 8, pp. 3768–3774, Aug. 2015.
[130] R. Singha and D. Vakula, "Directive beam of the monopole antenna using broadband gradient refractive index metamaterial for ultra-wideband application," *IEEE Access*, vol. 5, pp. 9757–9763, 2017.
[131] X. Chen, H. F. Ma, X. Y. Zou, W. X. Jiang, and T. J. Cui, "Three-dimensional broadband and high-directivity lens antenna made of metamaterials," *J. Appl. Phys.*, vol. 110, no. 4, pp. 044904-1–044904-8, Aug. 2011.
[132] X. Su, A. N. Norris, C. W. Cushing, M. R. Haberman, and P. S. Wilson, "Broadband focusing of underwater sound using a transparent pentamode lens," *J. Acoust. Soc. Amer.*, vol. 141, no. 6, pp. 4408–4417, Jun. 2017.
[133] M. Q. Qi, W. X. Tang, H. F. Ma, B. C. Pan, Z. Tao, Y. Z. Sun, and T. J. Cui, "Suppressing side-lobe radiations of horn antenna by loading metamaterial lens," *Sci. Rep.*, vol. 5, no. 1, pp. 1–6, Aug. 2015.
[134] D. R. Smith, J. J. Mock, A. F. Starr, and D. Schurig, "Gradient index metamaterials," *Phys. Rev. E, Stat. Phys. Plasmas Fluids Relat. Interdiscip. Top.*, vol. 71, no. 3, pp. 1–6, Mar. 2005.
[135] F.-Y. Meng, R.-Z. Liu, K. Zhang, D. Erni, Q. Wu, L. Sun, and J. L.-W. Li, "Automatic design of broadband gradient index metamaterial lens for gain enhancement of circularly polarized antennas," *Prog. Electromagn. Res.*, vol. 141, pp. 17–32, 2013.
[136] R. Singha and D. Vakula, "Gain enhancement of the ultra-wideband tapered slot antenna using broadband gradient refractive index metamaterial," *Int. J. RF Microw. Comput.-Aided Eng.*, vol. 28, no. 2, pp. 1–10, 2017.
[137] H.-X. Xu, G.-M. Wang, Z. Tao, and T. J. Cui, "High-directivity emissions with flexible beam numbers and beam directions using gradient-refractive-index fractal metamaterial," *Sci. Rep.*, vol. 4, no. 1, pp. 1–10, May 2015.
[138] B. P. Mishra, S. Sahu, S. K. S. Parashar, and S. K. Pathak, "A compact wideband and high gain GRIN metamaterial lens antenna system suitable for C, X, Ku band application," *Optik*, vol. 165, pp. 266–274, Jul. 2018.
[139] A. Dhouibi, S. N. Burokur, A. D. Lustrac, and A. Priou, "Low-profile substrate-integrated lens antenna using metamaterials," *IEEE Antennas Wireless Propag. Lett.*, vol. 12, pp. 43–46, 2013.
[140] A. K. Panda, S. Sahu, and R. K. Mishra, "DRA gain enhancement using a planar metamaterial superstrate," *Int. J. RF Microw. Comput.-Aided Eng.*, vol. 28, no. 7, pp. 1–10, 2018.
[141] A. K. Pandey, M. Chauhan, V. K. Killamsety, and B. Mukherjee, "High-gain compact rectangular dielectric resonator antenna using metamaterial as superstrate," *Int. J. RF Microw. Comput.-Aided Eng.*, vol. 29, no. 12, pp. 1–10, Dec. 2019.
[142] A. R. H. Alhawari, A. Ismail, M. A. Mahdi, and R. S. A. R. Abdullah, "Antipodal Vivaldi antenna performance booster exploiting snug-in negative index metamaterial," *Prog. Electromagn. Res. C*, vol. 27, pp. 265–279, 2012.
[143] M. J. Jeong, N. Hussain, J. W. Park, S. G. Park, S. Y. Rhee, and N. Kim, "Millimeter-wave microstrip patch antenna using vertically coupled split ring metaplate for gain enhancement," *Microw. Opt. Technol. Lett.*, vol. 61, no. 10, pp. 2360–2365, Oct. 2019.

[144] C. Arora, S. S. Pattnaik, and R. N. Baral, "Performance enhancement of patch antenna array for 5.8 GHz Wi-MAX applications using metamaterial inspired technique," *AEU-Int. J. Electron. Commun.*, vol. 79, pp. 124–131, Sep. 2017.
[145] H. A. Majid, M. K. A. Rahim, and T. Masri, "Microstrip antenna's gain enhancement using left-handed metamaterial structure," *Prog. Electromagn. Res. M*, vol. 8, pp. 235–247, 2009.
[146] C. Arora, S. S. Pattnaik, and R. N. Baral, "SRR superstrate for gain and bandwidth enhancement of microstrip patch antenna array," *Prog. Electromagn. Res. B*, vol. 76, pp. 73–85, 2017.
[147] E. C. Moreira, R. O. Martins, B. M. S. Ribeiro, and A. S. B. Sombra, "A novel gain-enhanced antenna with metamaterial planar lens for long-range UHF RFID applications," *Prog. Electromagn. Res. B*, vol. 85, pp. 143–161, 2019.
[148] M. Luo, X. Sang, J. Tan, and J. Chen, "A novel miniaturized metamaterial lens antenna," *Int. J. RF Microw. Comput.-Aided Eng.*, vol. 30, no. 7, pp. 1–8, Jul. 2020.
[149] X. Chen, J. Chen, C. Liu, and K. Huang, "A genetic metamaterial and its application to gain improvement of a patch antenna," *J. Electromagn. Waves Appl.*, vol. 26, nos. 14–15, pp. 1977–1985, Oct. 2012.
[150] R. Mark, N. Rajak, K. Mandal, and S. Das, "Metamaterial based superstrate towards the isolation and gain enhancement of MIMO antenna for WLAN application," *AEU-Int. J. Electron. Commun.*, vol. 100, pp. 144–152, Feb. 2019.
[151] N. Gupta, J. Saxena, K. S. Bhatia, and N. Dadwal, "Design of metamaterial-loaded rectangular patch antenna for satellite communication applications," *Iranian J. Sci. Technol., Trans. Electr. Eng.*, vol. 43, no. S1, pp. 39–49, Jul. 2019.
[152] S. Roy and U. Chakraborty, "Gain enhancement of a dual-band WLAN microstrip antenna loaded with diagonal pattern metamaterials," *IET Commun.*, vol. 12, no. 12, pp. 1448–1453, Jul. 2018.
[153] W. A. E. Ali, H. A. Mohamed, A. A. Ibrahim, and M. Z. M. Hamdalla, "Gain improvement of tunable band-notched UWB antenna using metamaterial lens for high speed wireless communications," *Microsyst. Technol.*, vol. 25, no. 11, pp. 4111–4117, Nov. 2019.
[154] M. Sarkar, R. Datta, P. Saha, and D. Mitra, "Design of a compact planar quasi-Yagi antenna with enhanced gain and bandwidth using metamaterial," *Prog. Electromagn. Res. Lett.*, vol. 62, pp. 125–131, 2016.
[155] M. Alibakhshi-Kenari, M. Naser-Moghadasi, and R. A. Sadeghzadeh, "Composite right–left-handed-based antenna with wide applications in very-high frequency–ultra-high frequency bands for radio transceivers," *IET Microw., Antennas Propag.*, vol. 9, no. 15, pp. 1713–1726, Dec. 2015.
[156] M. Alibakhshikenari, B. S. Virdee, A. Ali, and E. Limiti, "Miniaturised planar-patch antenna based on metamaterial L-shaped unit-cells for broadband portable microwave devices and multiband wireless communication systems," *IET Microw., Antennas Propag.*, vol. 12, no. 7, pp. 1080–1086, Jun. 2018.
[157] M. Alibakhshi-kenari, M. Naser-Moghadasi, R. A. Sadeghzadeh, B. S. Virdee, and E. Limiti, "Periodic array of complementary artificial magnetic conductor metamaterials-based multiband antennas for broadband wireless transceivers," *IET Microw., Antennas Propag.*, vol. 10, no. 15, pp. 1682–1691, Dec. 2016.

BASHAR A. F. ESMAIL (Member, IEEE) received the B.Eng. degree (Hons.) in electrical engineering (telecommunications) from Ibb University, Yemen, in 2008, and the M.Eng. and Ph.D. degrees in electrical engineering from Universiti Tun Hussein Onn Malaysia, Malaysia, in 2016 and 2021, respectively. He is currently working as a Postdoctoral Researcher with the Engineering Optimization and Modeling Center (EOMC), Department of Electrical Engineering, Reykjavik University, Iceland. His research interests include the areas of design of metamaterial structures, millimeter wave antenna, MIMO, and reconfigurable antennas.

SLAWOMIR KOZIEL (Fellow, IEEE) received the M.Sc. and Ph.D. degrees in electronic engineering from the Gdańsk University of Technology, Poland, in 1995 and 2000, respectively, and the M.Sc. degree in theoretical physics and the M.Sc. and Ph.D. degrees in mathematics from the University of Gdańsk, Poland, in 2000, 2002, and 2003, respectively. He is currently a Professor with the Department of Engineering, Reykjavik University, Iceland. His research interests include CAD and modeling of microwave and antenna structures, simulation-driven design, surrogate-based optimization, space mapping, circuit theory, analog signal processing, evolutionary computation, and numerical analysis.

STANISLAW SZCZEPANSKI received the M.Sc. and Ph.D. degrees in electronic engineering from the Gdańsk University of Technology, Poland, in 1975 and 1986, respectively. In 1986, he was a Visiting Research Associate with the Institut National Polytechnique de Toulouse (INPT), Toulouse, France. From 1990 to 1991, he was with the Department of Electrical Engineering, Portland State University, Portland, OR, USA, on the Kosciuszko Foundation Fellowship. From August 1998 to September 1998, he was a Visiting Professor with the Faculty of Engineering and Information Sciences, University of Hertfordshire, Hatfield, U.K. He is currently a Professor with the Department of Microelectronic Systems, Faculty of Electronics, Telecommunications and Informatics, Gdańsk University of Technology. He has published more than 160 papers and holds three patents. His teaching and research interests include circuit theory, fully integrated analog filters, high-frequency transconductance amplifiers, analog integrated circuit design, and analog signal processing.